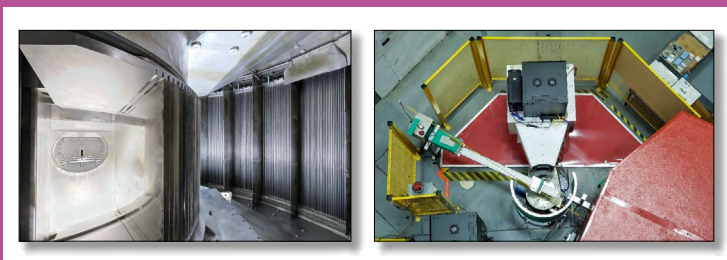


Thermal Scattering Law **S**(α, β): Measurement, Evaluation and Application

International Evaluation
Co-operation Volume 42



Nuclear Science

Thermal Scattering Law $S(\alpha, \beta)$: Measurement, Evaluation and Application

International Evaluation Co-operation Volume 42

© OECD 2020
NEA No. 7511

NUCLEAR ENERGY AGENCY
ORGANISATION FOR ECONOMIC CO-OPERATION AND DEVELOPMENT

ORGANISATION FOR ECONOMIC CO-OPERATION AND DEVELOPMENT

The OECD is a unique forum where the governments of 36 democracies work together to address the economic, social and environmental challenges of globalisation. The OECD is also at the forefront of efforts to understand and to help governments respond to new developments and concerns, such as corporate governance, the information economy and the challenges of an ageing population. The Organisation provides a setting where governments can compare policy experiences, seek answers to common problems, identify good practice and work to co-ordinate domestic and international policies.

The OECD member countries are: Australia, Austria, Belgium, Canada, Chile, the Czech Republic, Denmark, Estonia, Finland, France, Germany, Greece, Hungary, Iceland, Ireland, Israel, Italy, Japan, Latvia, Lithuania, Luxembourg, Mexico, the Netherlands, New Zealand, Norway, Poland, Portugal, Korea, the Slovak Republic, Slovenia, Spain, Sweden, Switzerland, Turkey, the United Kingdom and the United States. The European Commission takes part in the work of the OECD.

OECD Publishing disseminates widely the results of the Organisation's statistics gathering and research on economic, social and environmental issues, as well as the conventions, guidelines and standards agreed by its members.

*This work is published under the responsibility of the Secretary-General of the OECD.
The opinions expressed and arguments employed herein do not necessarily reflect the official
views of the Organisation or of the governments of its member countries.*

NUCLEAR ENERGY AGENCY

The OECD Nuclear Energy Agency (NEA) was established on 1 February 1958. Current NEA membership consists of 33 countries: Argentina, Australia, Austria, Belgium, Canada, the Czech Republic, Denmark, Finland, France, Germany, Greece, Hungary, Iceland, Ireland, Italy, Japan, Luxembourg, Mexico, the Netherlands, Norway, Poland, Portugal, Korea, Romania, Russia, the Slovak Republic, Slovenia, Spain, Sweden, Switzerland, Turkey, the United Kingdom and the United States. The European Commission and the International Atomic Energy Agency also take part in the work of the Agency.

The mission of the NEA is:

- to assist its member countries in maintaining and further developing, through international co-operation, the scientific, technological and legal bases required for a safe, environmentally sound and economical use of nuclear energy for peaceful purposes;
- to provide authoritative assessments and to forge common understandings on key issues as input to government decisions on nuclear energy policy and to broader OECD analyses in areas such as energy and the sustainable development of low-carbon economies.

Specific areas of competence of the NEA include the safety and regulation of nuclear activities, radioactive waste management and decommissioning, radiological protection, nuclear science, economic and technical analyses of the nuclear fuel cycle, nuclear law and liability, and public information. The NEA Data Bank provides nuclear data and computer program services for participating countries.

This document, as well as any [statistical] data and map included herein, are without prejudice to the status of or sovereignty over any territory, to the delimitation of international frontiers and boundaries and to the name of any territory, city or area.

Corrigenda to OECD publications may be found online at: www.oecd.org/about/publishing/corrigenda.htm.

© OECD 2020

You can copy, download or print OECD content for your own use, and you can include excerpts from OECD publications, databases and multimedia products in your own documents, presentations, blogs, websites and teaching materials, provided that suitable acknowledgement of the OECD as source and copyright owner is given. All requests for public or commercial use and translation rights should be submitted to neapub@oecd-nea.org. Requests for permission to photocopy portions of this material for public or commercial use shall be addressed directly to the Copyright Clearance Center (CCC) at info@copyright.com or the Centre français d'exploitation du droit de copie (CFC) contact@cfcopies.com.

Cover photos: The Institut Laue-Langevin reactor in Genoble, France (CEA, France); The North Carolina State University PULSTAR reactor neutron powder diffraction instrument (NCSU, United States).

Foreword

Understanding nuclear physics, or the study of atomic nuclei and their interactions, is essential in the modelling of all nuclear systems. Nuclear reactors using water or graphite moderators as well as other nuclear systems rely on low-energy neutrons that produce virtually all of the fission or other vital nuclear reactions in the system. The interaction of low-energy neutrons with matter – including with the moderators, structural materials and fuel – comprises complex scattering phenomena that are the subject of a field of research known as thermal neutron scattering. Dedicated scientific programmes around the world prepare precise nuclear data libraries of these scattering properties.

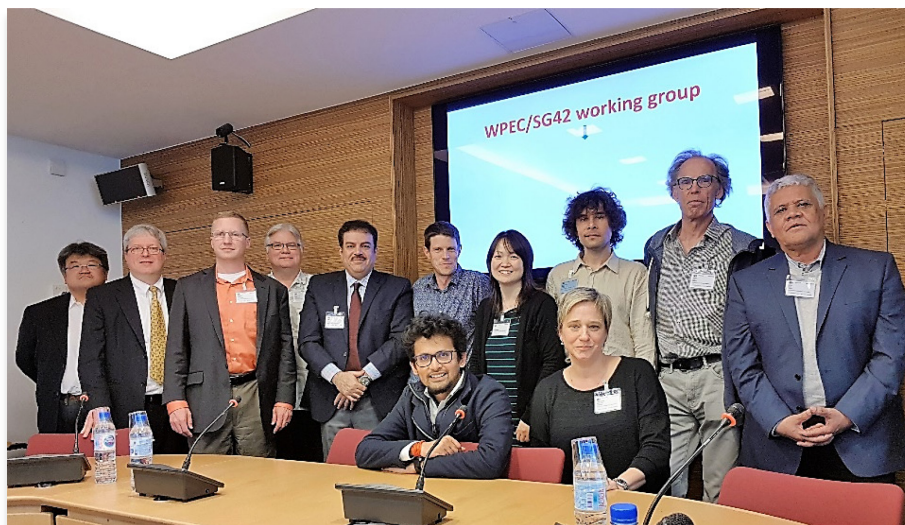
The OECD Nuclear Energy Agency (NEA) Working Party on International Nuclear Data Evaluation Co-operation (WPEC) was established under the NEA Nuclear Science Committee (NSC) in 1989 to promote the exchange of information on nuclear data evaluations, validation and related topics. Its aim is also to provide a framework for co-operative activities among members of the major nuclear data evaluation projects. This framework includes the possible exchange of scientists in order to encourage co-operation. The WPEC determines common criteria for evaluated nuclear data files with a view to assessing and improving the quality and completeness of evaluated data.

The WPEC is overseen by the NEA in close co-operation with several parties, such as the Russian Evaluated Neutron Data Library (BROND), the Evaluated Nuclear Data File (ENDF, United States), the Japanese Evaluated Nuclear Data Library (JENDL), the Joint Evaluated Fission and Fusion File (JEFF) (with other NEA Data Bank member countries) and the Chinese Evaluated Nuclear Data Library (CENDL) through the Nuclear Data Section of the International Atomic Energy Agency (IAEA).

The present report provides an overview of activities undertaken by the WPEC/Subgroup 42 (SG 42) on thermal scattering kernel $S(\alpha, \beta)$: measurement, evaluation and application. The SG 42 has studied the thermal neutron scattering law (TSL) and the cross-section evaluation process, ultimately contributing to the new evaluations of thermal scattering data that have been adopted in the most recent evaluations of the American ENDF/B-VIII.0 and NEA Data Bank JEFF-3.3 nuclear data libraries. This report summarises results on thermal scattering data and outlines plans for the next phase of collaboration.

Acknowledgements

The Nuclear Energy Agency would like to acknowledge the contributions of the members of the Working Party on International Nuclear Data Evaluation Co-operation (WPEC)/Subgroup 42 (SG 42) to this report. A photograph of the attendees/members of the closing meeting is shown below.



Members of the SG 42 attending the last meeting of the group in May 2018, at the NEA Headquarters in Boulogne-Billancourt, France, from left to right: Atsushi Kimura (Japan Atomic Energy Agency), Michael Zerkel (Naval Nuclear Laboratory, United States), Jesse Holmes (Naval Nuclear Laboratory, United States), David Heinrichs (Lawrence Livermore National Laboratory, United States), Ayman Hawari (SG 42 Monitor, North Carolina State University, United States), Gilles Noguere (SG 42 Co-ordinator, French Alternative Energies and Atomic Energy Commission [CEA /DEN] Cadarache, France), Li (Emily) Liu (Rensselaer Polytechnic Institute [RPI], United States), Danila Roubtsov (Canadian Nuclear Laboratories), Ivo Kodeli (Josef Stefan Institute, Slovenia), Luiz Leal (Institut de Radioprotection et de Sûreté Nucléaire [IRSN], Fontenay-aux-Roses, France), Vaibhav Jaiswal (seated, IRSN, Fontenay-aux-Roses, France), Florencia Cantargi (seated, Centro Atómico Bariloche [CAB], Argentina). Other contributing members who are not in the photo include but are not limited to: Yaron Danon (RPI, United States) and Jose Ignacio Márquez Damián (CAB, Argentina).

Table of contents

List of abbreviations and acronyms	7
Executive summary	9
Chapter 1. Introduction	11
Chapter 2. Theory: Evaluation methods and tools	13
2.1. Thermal scattering law definition.....	14
2.2. Methodology of TSL generation using NJOY/LEAPR	14
2.3. Use of atomistic simulations to support TSL analysis	17
2.4. Future developments in TSL evaluation and processing.....	21
Chapter 3. Experimental validation	27
3.1. Experimental programme at North Carolina State University.....	27
3.2. Experimental programmes at Spallation Neutron Source (ORNL, United States).....	32
3.3. Experimental programmes at the Institut Laue-Langevin (Grenoble, France)	33
3.4. Experimental Programme for Centro Atómico Bariloche and collaborators.....	34
3.5. Integral experiments	37
3.6. Facilities for TSL experiments and capability gaps	39
Chapter 4. Thermal scattering law data format and uncertainty issues	41
4.1. Modern TSL library format	41
4.2. TSL uncertainties	46
Chapter 5. Summary and recommendations	49
References	51

List of figures

2.1. A representation of the double-differential thermal neutron scattering cross-section of uranium dioxide (UO ₂).....	15
2.2. A comparison of the measured TSL and the calculated TSL for beryllium metal....	16
2.3. Width of the quasielastic peak in light water as a function of the change in neutron wavevector	16
2.4. The top plot is a flowchart of TSL analysis based on input generated using <i>ab initio</i> DFT and lattice dynamics methods	18
2.5. A schematic of TSL analysis based on input generated using <i>ab initio</i> methods and the neutron scattering experimental data from indirect neutron geometry spectrometer, like VISION at SNS	19
2.6. Total scattering cross-section of liquid para-hydrogen and liquid ortho-deuterium at 19 K.....	21
2.7. A demonstration of the input and diagnostic interfaces of the FLASSH code.....	22
2.8. A comparison of the measured TSL and the calculated TSL for beryllium metal....	23
2.9. FLASSH analysis capturing coherent inelastic interference and showing a 3D view of the symmetric $S(\alpha,\beta)$ for aluminium above a minimum threshold for α and β	23

2.10.	Total neutron cross-section for metallic copper computed with NCrystal, compared with experimental data from EXchange FORmat (EXFOR)	24
2.11.	Calculation of the total cross-section of metallic beryllium using NJOY and NJOY-NCrystal compared with ENDF/B-VIII.0	24
3.1.	Hierarchy of validation levels for thermal scattering libraries	27
3.2.	PAS and NPD measurements performed at the NCSU PULSTAR reactor on unirradiated and irradiated “nuclear” graphite samples	28
3.3.	Examples of thermodynamic properties as a function of the temperature ($T < 350$ K) used to validate <i>ab initio</i> calculations for Yttrium hydride (YH_2)	29
3.4.	Measured $G(Q,E)$ contours for “nuclear” graphite	30
3.5.	Nuclear graphite measured and calculated (using <i>ab initio</i> atomistic simulations) GDOS	30
3.6.	The total cross-section of nuclear graphite measured using nine angstrom (1 meV) neutrons at the National Institute of Standards and Technology reactor	31
3.7.	A comparison of the measured and predicted detector response in the NCSU PSDT experiment performed in a graphite pile at the Oak Ridge Electron Linear Accelerator (ORELA) facility	32
3.8.	Comparison of VISION $S(Q, \omega)$ and $S(Q, \omega)$ calculated using CASTEP and oClimax after the locations of the peaks have been adjusted to match the experimental data	33
3.9.	Comparison of the experimental DDSCS from ARCS at 250 meV incident neutron energy and DDSCS calculated using oClimax derived phonon spectrum with NJOY-2016	33
3.10.	Temperature dependence of the total thermal neutron cross-section of heavy water as a function of energy	34
3.11.	Temperature dependence of the total thermal neutron cross-section of light water as a function of energy, shown as the ratio of the total cross-section at 473 and 293 K	35
3.12.	Temperature dependence of the total thermal neutron cross-section of light water as a function of energy, shown as the difference of the total cross-section at 353 and 283 K	35
3.13.	Experimental total neutron cross-section data sets for light water measured at different temperatures	36
3.14.	Multiplication factor of ICSBEP plutonium solution benchmarks as a function of the energy of average neutron lethargy causing fission (EALF) calculated using ENDF/B-VII.1 and ENDF/B-VIII.0	37
3.15.	Differences between calculated (C) and experimental (E) reactivity obtained as a function of the temperature in the framework of the MISTRAL-1 programme carried out in the EOLE facility (CEA Cadarache)	38
3.16.	Thermal flux time decay eigenvalues vs. buckling for liquid water spheres with selected thermal neutron scattering kernels	39
4.1.	An example of “Option 1” for the GNDS format of TSL data	43
4.2.	An example of “Option 2” for the GNDS format of TSL data	44
4.3.	An example of “Option 3” for the GNDS format of TSL data	45
4.4.	Double-differential scattering cross-sections for light water calculated with JEFF-3.1.1 (Mattes’ model) and compared with data measured by Bischoff et al. (1967) at the Rensselaer Polytechnic Institute (RPI) facility	47

List of tables

2.1.	A comparison between the major features of NJOY and FLASSH for TSL evaluation	22
4.1.	New and updated TSL libraries in the ENDF/B-VIII.0 and JEFF-3.3 releases contributed by NCSU, CAB, CNL and BAPL	42

List of abbreviations and acronyms

ARCS	Wide Angular-Range Chopper Spectrometer
CAB	Centro Atómico Bariloche
CEA	French Alternative Energies and Atomic Energy Commission
DDSCS	Double-differential scattering cross-section
DFT	Density functional theory
(v)(G)DOS	(Virtual) (generalised) density of states
ENDF	Evaluated Nuclear Data File
EOLE	Low power experimental reactor for neutron studies
ESS	European Spallation Source
EXFOR	EXchange FORmat
FLASSH	Full Law Analysis Scattering System Hub
GNDS	Generalised Nuclear Data Structure
IAEA	International Atomic Energy Agency
ICSBEP	International Criticality Safety Benchmark Evaluation Project
ILL	Institut Laue-Langevin
JEFF	Joint Evaluated Fission and Fusion File
LEAPR	Module of the NJOY processing code for thermal neutron scattering data
MD	Molecular dynamics
NEA	Nuclear Energy Agency
NCSU	North Carolina State University (United States)
NPD	Neutron powder diffraction
OECD	Organisation for Economic Co-operation and Development
ORNL	Oak Ridge National Laboratory (United States)
PAS	Positron annihilation spectroscopy
PNDA	Pulsed neutron die away
PSDT	Pulsed slowing-down time
RPI	Rensselaer Polytechnic Institute
SG	Subgroup
SNS	Spallation Neutron Source (Oak Ridge National Laboratory, United States)
TSL	Thermal scattering law
UN	Uranium nitride
WPEC	Working Party on International Nuclear Data Evaluation Co-operation (NEA)

Executive summary

The simulation of nuclear systems requires a variety of data, which depend on the typical energies of the active particles. For many well-known systems, such as light water, heavy water or graphite-moderated nuclear reactors, cold neutron source facilities (e.g. spallation neutron sources) and others, neutrons are slowed down to low energies where the chemical structure of materials plays a central role in the neutron physics. The simulation of thermalised neutronic systems is highly sensitive to neutron scattering. The evaluation and validation of these data are therefore of great importance and represent a specialised discipline within the nuclear data community. Over the past two decades, great advances have been made in the use of atomistic simulation techniques, including density functional theory (DFT) and molecular dynamics (MD) that, alongside the increase in computational power, have provided a wealth of theoretical information for thermal scattering law (TSL) evaluations. Combined with new experimental data obtained in the past decade, these advances have resulted in an active area of research. A subgroup was launched in 2015 under the OECD Nuclear Energy Agency (NEA) Working Party on International Nuclear Data Evaluation Co-operation (WPEC) to co-ordinate international activities in this area.

The work of this subgroup has stimulated numerous activities, directly or indirectly resulting in a suite of new evaluated TSL data evaluations that have been adopted in the most recent nuclear data libraries of the United States (Evaluated Nuclear Data File [ENDF]/B-VIII.0, February 2018) and the NEA Data Bank (Joint Evaluated Fission and Fusion File [JEFF]-3.3, November 2017). Activities include new evaluations for novel materials such as uranium nitride (UN), silicon carbide (SiC), silicon oxide (SiO₂) and aluminium oxide (Al₂O₃), as well as the re-evaluation of critical materials, including water (H₂O) and heavy water (D₂O), and enhanced evaluations, including graphite at multiple levels of porosity and phase I_h ice. Using the new evaluation techniques, opportunities to provide additional data that were previously unavailable – including correlated uncertainties – have been explored. New frontiers have been established through Subgroup 42, including the development and utilisation of new data, the application of novel techniques to modern neutronic systems and the use of the most recent experimental data, which will be addressed in future WPEC activities.

Chapter 1. Introduction

The physics of nuclear reactions includes essential information for the design, operation and decommissioning of nuclear systems, with applications spanning energy, safety, medicine, science, security and a great many other industrial processes. In order to simulate and understand the physics of facilities, a comprehensive knowledge of the relevant nuclear physics is required. This generally involves an understanding of the physics of particles, such as neutrons, at energies that range from millions of electronvolts (MeV), where they are created in fission processes or accelerators, down to sub-eV energies found at room temperature and lower. The basic principle of virtually all commercial nuclear power plants in operation is to reduce the energy of fission neutrons by a factor of more than 1 million so as to take advantage of the large uranium and plutonium fission probabilities at these low energies.

The nature of the physics of nuclear reactions is fundamentally different between MeV and sub-eV energies. Above a few eV, neutron transport is insensitive to chemical structures and materials are treated as regions without any atomic-level order. At lower energies, molecular excitations (e.g. rotations or vibrations) and collective excitations, known as phonons, are crucial to the understanding of how neutrons interact with the material. As a result, H₂O cannot be treated as simply a mixture of hydrogen and oxygen atoms, but must be seen as hydrogen and oxygen specifically bound within water molecules. The phase of the material, whether it be liquid, gas or any one of potentially numerous possible solid phases, must also be known. If there are defects (e.g. graphite with a given porosity), the density of these defects must be considered as well. Even the spin isomeric states must be considered for elemental hydrogen.

All of these factors contribute to how neutrons scatter within the material at low energies. This fact was appreciated in the earliest days of analysing thermalising nuclear systems, and the bespoke nuclear data sub-libraries were thus created to store thermal scattering law (TSL) data, known in the technical community as $S(\alpha,\beta)$, which ultimately is used to describe how scattering changes the energy and angle of incident neutrons. The related double-differential cross-section is crucial in understanding where thermal neutrons travel and what their energy spectrum looks like, which for obvious reasons is of considerable importance for systems such as thermal nuclear reactors, where thermal neutrons drive virtually all of the fission in the system.

The earliest TSL data from the 1960s, and the updated data made for the Evaluated Nuclear Data File (ENDF)/B-VI and ENDF/B-VII series of nuclear data libraries, relied upon many simplifying approximations, including an assumption that coherent inelastic scattering could be ignored. With the advent of sophisticated atomistic simulation methods and new experiments, the international nuclear data community now possesses the tools and data required to considerably improve TSL sub-libraries. During the process of updating TSL data, new evaluations have been made for materials such as ice, to address the needs of the criticality safety community in scenarios of cold climates, and high-porosity, unirradiated and irradiated nuclear graphite for use in advanced reactor applications.

Chapter 2 of this report briefly reviews the theory behind TSL data, and provides an overview of the legacy and novel techniques and tools used in its evaluation, including examples of limitations in the previous methods with comparisons against modern measurements. Chapter 3 describes the multifaceted validation exercises against

experimental data from multiple laboratories and against integral benchmarks from the International Criticality Safety Benchmark Evaluation Project (ICSBEP). Chapter 4 describes TSL data formats, the universal adoption of the new data in all major nuclear data library releases and new uncertainty data that will be integrated into an extended nuclear data format being developed in another expert group under the NEA Working Party on International Nuclear Data Evaluation Co-operation (WPEC).

Chapter 2. Theory: Evaluation methods and tools

Over the past 20 years, significant advances in the utility of atomistic simulation techniques, such as *ab initio* density functional theory (DFT) and molecular dynamics (MD) methods, made it possible to predictively calculate the properties of materials. It became clear to practitioners in the field of thermal neutron scattering as a consequence that such methods represent a major resource for supplying needed information (e.g. excitation density of states [DOS], atomistic correlation functions), for performing high-fidelity calculations of the thermal neutron scattering law and generating thermal scattering law (TSL) libraries (Hawari, 2014). This realisation also motivated further discussion on updating the computer codes and tools that are used in TSL calculations to take full advantage of the wealth of information that is available when using atomistic simulation methods. The Full Law Analysis Scattering System Hub (FLASSH) code is an example of a modern tool presented during the NEA Working Party on International Nuclear Data Evaluation Co-operation (WPEC)/Subgroup 42 (SG 42) meetings. The tool is capable of performing the TSL evaluation using traditional techniques (i.e. similar to the NJOY code) but also has the ability to relax many of the approximations. FLASSH is designed to support all TSL evaluation steps, including the use of DFT and/or MD generated input (Zhu and Hawari, 2018).

New TSL measurements for different materials have also been performed in the last ten years. Evaluation methodologies for generating TSL were then developed in parallel to take full advantage of these new data. As an example, this effort can be illustrated by the work of Ramić et al. (2018), in which experimental data are used to guide and validate TSLs. The methodology relies on the oClimax code, used for neutron vibrational spectral analysis (Ramirez-Cuesta, 2004). In that case, the new TSL, which is still created with NJOY, represents a TSL based on the DFT calculations but adjusted by the experimental data. In some cases, the NJOY code needs modifications to process the new evaluation.

Whatever the origins of the TSL, experimental validation is a crucial step in the evaluation procedure. Different types of experimental data of interest have been presented. Experimental needs, which emerged from the discussions, cover material properties (i.e. microstructure of the material), microscopic data (double-differential and total neutron cross-sections), semi-integral data (such as pulsed slowing-down-time [PSDT] experiments) and integral data. The latest item was illustrated with pulsed neutron die away (PNDA) benchmarks, temperature-dependent mock-up experiments for reactor applications carried out in the EOLE facility of the French Alternative Energies and Atomic Energy Commission (CEA) in Cadarache and the International Criticality Safety Benchmark Evaluation Project (ICSBEP) benchmarks for criticality purposes.

As improved evaluation methodologies have been developed, the modernisation of the TSL library format has become a necessity. In the nomenclature of the Evaluated Nuclear Data File (ENDF)-6 format, TSLs are currently stored in File MF=7 without the possibility of introducing covariances. In that context, opportunities offered by the Generalised Nuclear Data Structure (GNDS) structure are promising. Preliminary data format options are already available for testing. Storage options of covariances are still being debated, with the main issue being the size of the covariance matrices. For TSL, the size of the matrix can be significantly reduced by using an AGS-type (analysis of geel spectra) formalism or by directly using the covariance matrix between the model parameters. The second strategy is not always possible, and depends on the origin of the TSL evaluation. Both approaches were applied to the TSLs of light water.

2.1. Thermal scattering law definition

Neutrons interacting in a medium will undergo various absorption and scattering reactions with the nuclei of the medium. Initially, the scattering process will result in the neutrons losing energy and moderating (i.e. down scattering) until they reach a thermal energy limit set by the temperature of the medium. Once thermal, the neutrons will begin to undergo an energy exchange process with the medium's nuclei by which they may gain or lose energy (i.e. up and down scattering) until an "equilibrium" energy distribution is established. Neutrons in this "thermal" energy range, and through the thermal scattering, will begin to sample the dynamics and structure of the medium. To quantify this process, the double-differential cross-section for thermal neutron scattering is derived (Squires, 1978) based on first order perturbation theory (Born approximation) combined with a short ranged nuclear potential (Fermi pseudo potential) and is given by:

$$\frac{d^2\sigma}{d\Omega dE'} = \frac{1}{4\pi k_B T} \sqrt{\frac{E'}{E}} \left[\sigma_{coh} S(\alpha, \beta) + \sigma_{inc} S_s(\alpha, \beta) \right] \quad (1)$$

where $S(\alpha, \beta)$ is known as the TSL, and α and β represent dimensionless momentum and energy transfer variables, respectively. In addition, $S(\alpha, \beta)$ can be written as:

$$S(\alpha, \beta) = S_s(\alpha, \beta) + S_d(\alpha, \beta) \quad (2)$$

where S_s is known as the self-component of the scattering law and S_d is the distinct component of the scattering law. The TSL is directly proportional to the dynamic structure factor $S(\mathbf{Q}, \omega)$ of a given material, where \mathbf{Q} is the momentum transfer vector and ω is the frequency corresponding to energy transfer. In Van Hove's space-time representation (Van Hove, 1954), it was shown that $S(\mathbf{Q}, \omega)$ is the Fourier transform of particle density correlation functions. In space-time, these correlation functions can either represent the same particle at (\mathbf{r}, t) as was at $(0, 0)$, i.e. S_s , or a different particle at (\mathbf{r}, t) than that at $(0, 0)$, i.e. S_d . Consequently, independent of the interacting particle, the TSL is a property of the interaction medium that carries the information about its dynamics (momentum and energy states) and structure.

Due to its utility in computational analysis, several computer codes such as GASKET and NJOY have emerged during the past 60 years that are able to calculate $S(\alpha, \beta)$ (Koppel et al., 1967; MacFarlane et al., 2017; MacFarlane, 1994). In addition, $S(\alpha, \beta)$ is also tabulated in many nuclear data libraries, including the ENDF/B, Joint Evaluated Fission and Fusion File (JEFF) and the Japanese Evaluated Nuclear Data Library (JENDL). (Brown et al., 2018; NEA, 2017; Shibata et al., 2011). To date, the ENDF File 7 format continues to be the standard format for tabulating $S(\alpha, \beta)$ data and also for including elastic scattering data for a given material (CSEWG, 2010). However, all current calculations of $S(\alpha, \beta)$ are performed using several simplifying assumptions (see Section 2.2). In the last decade, it has nonetheless been shown that using input provided by atomistic simulation techniques, the TSL may be calculated predictively and with minimal simplifying assumptions, such as the incoherent approximation. Figure 2.1 summarises the previous discussion using UO_2 as an example material.

2.2. Methodology of TSL generation using NJOY/LEAPR

To date, the primary tool for generating the TSL in the ENDF File 7 format is the LEAPR module of the NJOY code (MacFarlane et al., 2017). LEAPR is primarily based on the incoherent approximation, which assumes that the distinct particle correlations

(interference effects) in the inelastic scattering process can be neglected (i.e. $S_d(\alpha, \beta) = 0$) resulting in the following expression for the double-differential cross-section:

$$\frac{d^2\sigma}{d\Omega dE'} = \frac{1}{4\pi k_B T} \sqrt{\frac{E'}{E}} (\sigma_{coh} + \sigma_{inc}) S_s(\alpha, \beta) \quad (3)$$

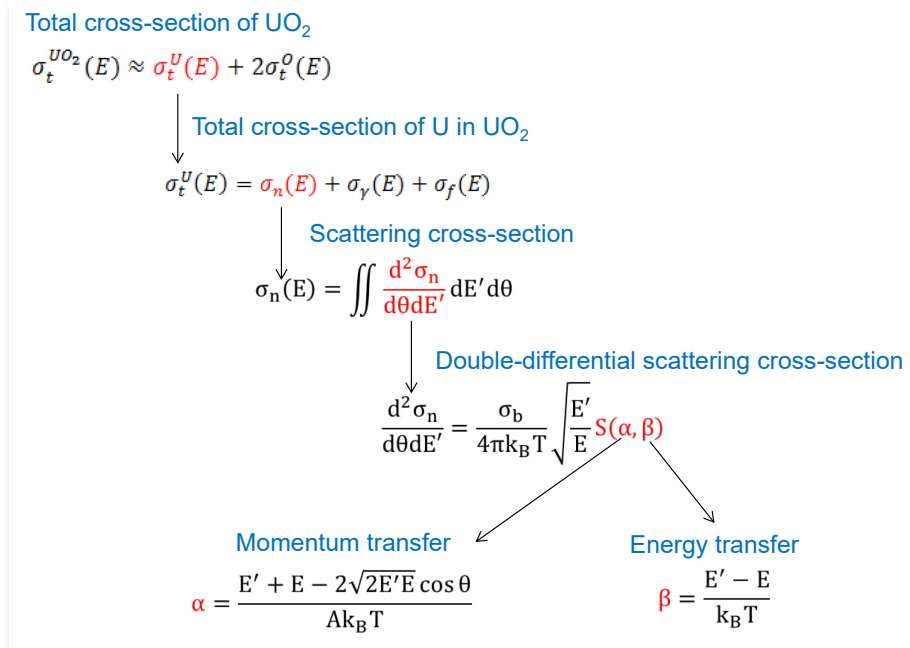
In addition, the LEAPR implementation is based on the formulation as given in typical references on thermal neutron scattering (Squires, 1978). Therefore, for solids, the TSL is calculated by assuming a Gaussian form for the density correlation function, a cubic atomic unit cell and a Bravais lattice that assumes one atom per unit cell.

LEAPR further applies a harmonic assumption, which allows for the application of the phonon expansion in the calculation of the double-differential scattering cross-section (DDSCS). In this case, Equation (3) may be written as:

$$\frac{d^2\sigma}{d\Omega dE'} = \frac{1}{4\pi k_B T} \sqrt{\frac{E'}{E}} (\sigma_{coh} + \sigma_{inc}) \sum_{p=1}^p S_s(\alpha, \beta) \quad (4)$$

where p is the phonon order representing the number of phonons created or annihilated in a scattering process.

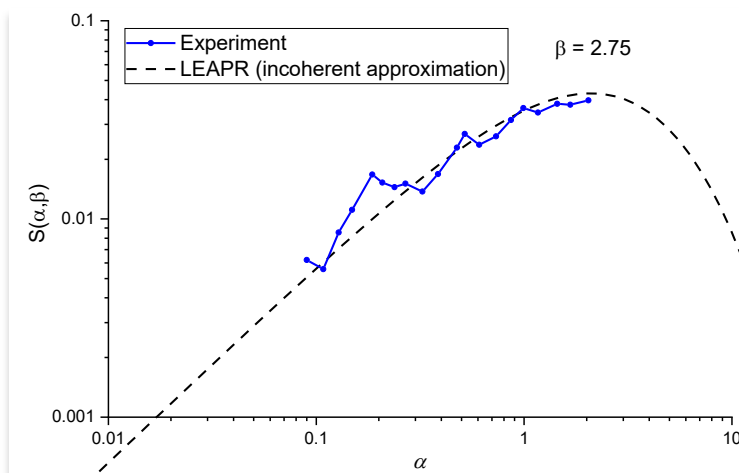
Figure 2.1. **A representation of the double-differential thermal neutron scattering cross-section of uranium dioxide (UO₂)**



For liquids, LEAPR assumes that the TSL is represented as the convolution of the partial TSL contributions due to different atomic and molecular excitation processes such as vibrations, rotations and translations. Therefore, to capture diffusive behaviour that becomes relevant in liquids, LEAPR applies a diffusion model to calculate the translational TSL and produces the total TSL by convolving the diffusion TSL with the TSL calculated in Equation (4). LEAPR also allows the calculation of the coherent inelastic component of the scattering law in liquids by applying the Sköld and Vineyard approximations.

The TSL as calculated by the standard version of LEAPR represents a reasonable approximation. However, comparison to measured data reveals that the LEAPR assumptions, especially the incoherent approximation, result in marked deviations from measured data (see Figure 2.2). Remedies to such deficiencies, including the incoherent approximation, have been presented through modern TSL evaluation tools such as the FLASSH code (Zhu and Hawari, 2018). In addition, the open source licence of NJOY allows for customisation, and versions have been developed to overcome some of these limitations (see Figure 2.3).

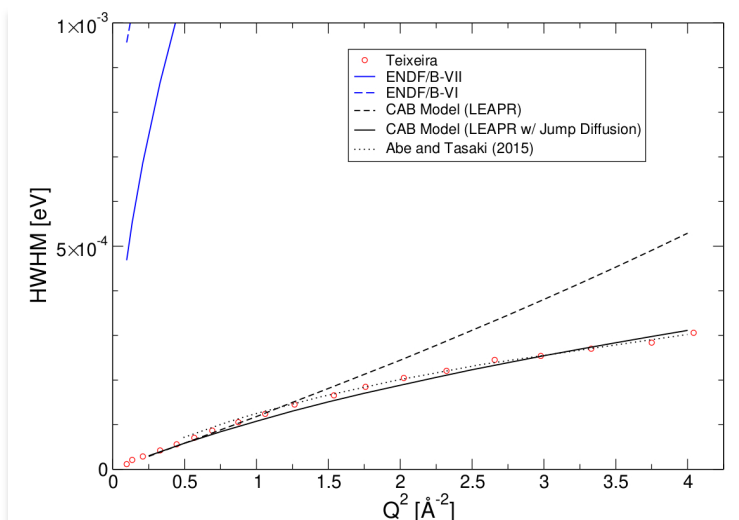
Figure 2.2. **A comparison of the measured TSL and the calculated TSL for beryllium metal**



Note: The calculation is performed using the LEAPR module of the NJOY code under the incoherent approximation [see Equation (3)].

Source: NCSU.

Figure 2.3. **Width of the quasielastic peak in light water as a function of the change in neutron wavevector**



Note: Calculations with the standard LEAPR module using a free gas translational model (ENDF/B-VI, ENDF/B-VII) show a significant discrepancy with the experimental data by Teixeira. The use of a the Egelstaff-Schofield diffusion model included in LEAPR improves the situation, but in order to match the experiment a jump diffusion model has to be introduced (Márquez Damián et al., 2016). This improved diffusion model has comparable results to the quantum correction model presented by Abe and Tasaki (2015).

Source: Márquez Damián et al., 2016.

2.3. Use of atomistic simulations to support TSL analysis

SG 42 participants presented new and improved evaluation methodologies during the meetings. Approaches used at various institutions are summarised below.

Methodology developed at North Carolina State University (NCSU)

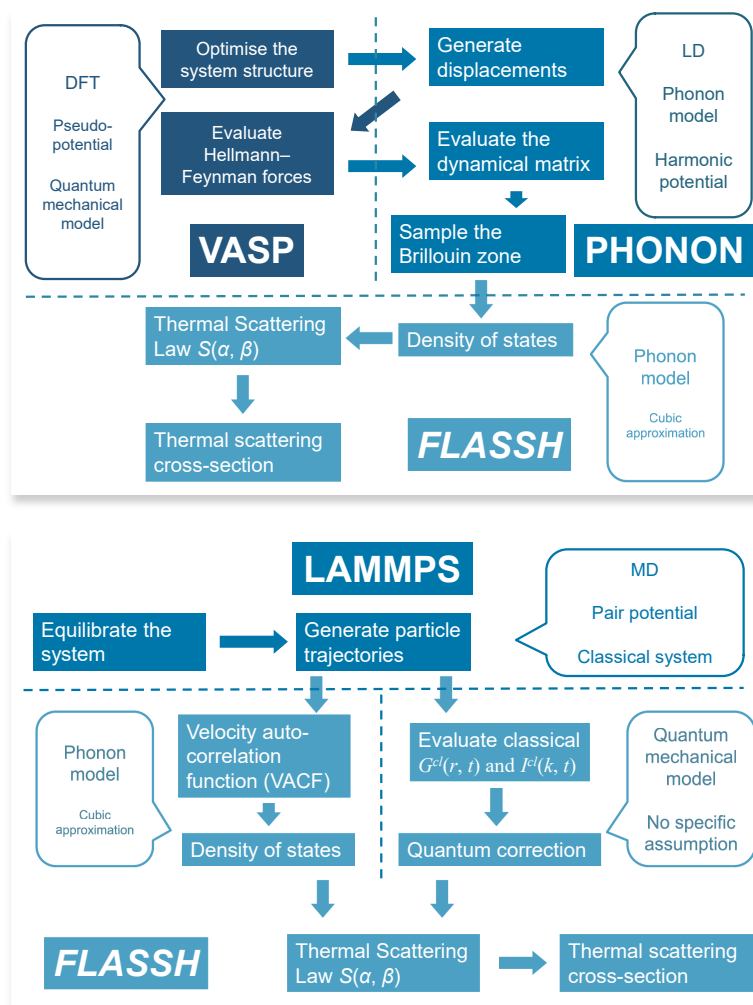
As described above, calculations of the TSL, $S(\alpha, \beta)$ are based on the space-time view of the scattering medium. In fact, even the LEAPR methodology produces the scattering law by assuming a Gaussian form for the self-atomic density autocorrelation function and the resulting intermediate scattering function. This produces a formulation where the primary input for the calculation is the phonon (vibrational) density of states (vDOS) for the system. In this case, the vDOS was either obtained from published literature, or calculated using simplistic atomistic models, where the forces are described by empirical fits to thermo-physical data and combined with classical dynamical matrix analysis to arrive at the vibrational frequency dispersion relations and in turn construct the vDOS (i.e. $\rho(\omega)$).

Early in this century, it was demonstrated that quantum mechanical calculations in the form of predictive atomistic simulations that implement *ab initio* DFT can be used to calculate the force field in an atomic system (Hawari et al., 2004). Overall, the DFT approach is implemented within the adiabatic Born-Oppenheimer approximation, where decoupling of the electronic and nuclear components in atomic systems is assumed. In return, DFT assumes that the total energy of the system can be set as a functional of the electronic density, which allows for an estimation of the ground state energy and the corresponding Hamiltonian. Subsequently, by implementing the Hellmann-Feynman theory, interatomic forces may be calculated. At this stage, use is again made of classical dynamical matrix analysis, which produces the frequency dispersion information and enables the construction of the vDOS by random sampling of the first Brillouin zone of the atomic system. The vDOS produced can then be used in a code such as LEAPR to produce a TSL evaluation. Over the past decade, this approach, which combines DFT with classical dynamical matrix analysis, has become computationally convenient to use for supporting the TSL evaluation process. However, it remains somewhat restrictive as it assumes no temperature dependence of the vDOS (the analysis inherently assumes behaviour at 0 K) and, as dictated by the dynamical matrix approach, it assumes harmonic behaviour of the system. Moreover, it is primarily suited for implementation in analysing crystalline periodic solids. DFT and dynamical matrix analysis tools that have been used in TSL evaluation include the VASP (Vienna *ab initio* simulation package) and PHONON codes (Kresse and Furthemüller, 1996a; Kresse and Furthemüller, 1996b; Parlinski et al., 1997). Figure 2.4 shows a schematic of the analysis steps and common tools that are used to produce a TSL.

Alternatively, classical MD techniques have been implemented to support TSL analysis (Manring and Hawari, 2019; Márquez Damián et al., 2014; Abe et al., 2014). MD is also implemented within the adiabatic Born-Oppenheimer approximation and uses Newtonian mechanics to track the motion of nuclei in the atomic system. In this approach, however, the interatomic electronic forces are estimated using empirical potential functions that are parameterised using the thermo-physical properties (e.g. density, thermal conductivity, viscosity) of a given material. While the parametrisation process can be tedious, the primary advantage of these techniques is that the calculation is temperature dependent, which inherently accounts for anharmonic effects that increase with temperature. In addition, the simulations approach can easily accommodate calculations that support all the typical states of matter: solid, liquid and gas. The MD approach uses atomistic correlations either to produce the generalised DOS for utilisation in a TSL evaluation code such as LEAPR or to calculate the TSL. In the latter option, the TSL produced represents a classical manifestation that requires the implementation of quantum corrections. Such corrections are needed to account for the treatment of the position variable classically as opposed to being a Heisenberg (quantum mechanical) operator. This restores the detailed balance and recoil

phenomena that are ignored in classical treatment. Nonetheless, the TSL produced using this approach will be inherently free from any theoretical artefacts such as LEAPR's incoherent approximation. MD codes that have been used to support recent TSL evaluations include LAMMPS and GROMACS (Plimpton, 1995; Berendsen et al., 1995). Figure 2.4 (bottom plot) illustrates the calculation steps when LAMMPS is used.

Figure 2.4. **The top plot is a flowchart of TSL analysis based on input generated using ab initio DFT and lattice dynamics methods**



Note: The codes VASP (DFT), PHONON (lattice dynamics) and FLASSH are examples of tools that can be used for TSL analysis. The bottom plot is for molecular dynamics simulations when the LAMMPS code is used.

Source: NCSU.

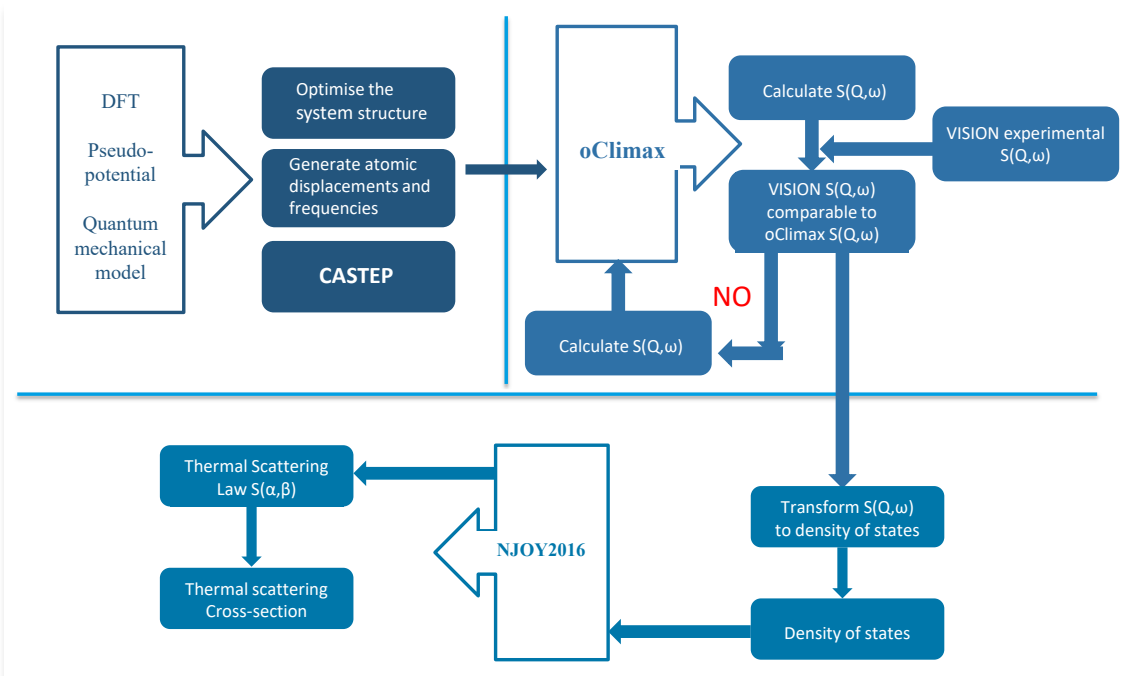
Methodology used at the Rensselaer Polytechnic Institute (RPI)

Because of the lack of experimental data for the validation of the current thermal scattering libraries for different moderators of interest to nuclear criticality safety, inelastic neutron scattering experiments have been performed. As described by Ramić et al. (2018), the experiments were performed at the Spallation Neutron Source (SNS) at Oak Ridge National Laboratory (ORNL) using two different types of spectrometers: indirect geometry (VISION)

and direct geometry (ARCS and SEQUOIA) neutron spectrometers. The data from ARCS and VISION spectrometers have been used in two manners:

- The experimental data in the form of DDSCS measurements at different incident energies and scattering angles has been used for comparison and validation of thermal scattering libraries created with NJOY-2016. The ARCS experimental set-up has been simulated using Monte Carlo N-Particle Transport Code (MCNP)6.1 to compare TSL evaluations with experiment.
- Using code oClimax, the output of the DFT calculations could be directly re-calculated to $S(Q, \omega)$ and compared to the observed $S(Q, \omega)$ using the VISION spectrometer. Furthermore, oClimax offers additional advantages due to the capability of oClimax to calculate partial contributions of each atom to the whole molecule generalised (G)DOS, while at the same time being capable of calculating the fundamental vibrational mode ($n=1$) and multiple phonon scattering contributions ($n>1$ overtones). The expected input for NJOY-2016 is the fundamental vibrational ($n=1$) DOS. The oClimax enables scaling of frequencies in $S(Q, \omega)$ spectra to correct the mismatch created by the structural differences of the experimental sample and how the material is simulated using DFT (see Figure 2.5). This methodology results in true experimental phonon spectrum from which any phonon related quantities can be calculated, such as the scattering law, specific heat capacity and thermal conductivity. The experimental polyethylene has semi-crystalline structure, for example, while in DFT calculations polyethylene is treated as a perfect crystal, possessing orthorhombic unit cell with space group Pnam.

Figure 2.5. A schematic of TSL analysis based on input generated using *ab initio* methods and the neutron scattering experimental data from indirect neutron geometry spectrometer, like VISION at SNS



Note: The codes CASTEP, oClimax and NJOY-2016 are examples of tools that can be used for TSL analysis.

Source: RPI.

Methodology used at Centro Atómico Bariloche

The Neutron Physics Department at Centro Atómico Bariloche (CAB) approaches thermal scattering evaluation using a heuristic methodology. This methodology implies the following steps:

- study of the material structure and dynamics, in terms of its interaction with neutrons;
- development of a physical model, in terms of an intermediate scattering function, $\chi(\bar{Q}, t)$;
- implementation of the model in the energy space;
- validation and verification of the model using differential and integral neutron scattering data and benchmarks experiments.

To illustrate this methodology, an overview is provided of the evaluation procedure used to generate the new TSL for liquid hydrogen and deuterium, which were contributed to JEFF-3.3.

The scattering law can be expressed as the Fourier transform of the intermediate scattering function:

$$S(\bar{Q}, \omega) = \frac{1}{2\pi\hbar} \int_{-\infty}^{\infty} dt e^{-i\omega t} \chi(\bar{Q}, t) \quad (5)$$

where we can write:

$$\chi(\bar{Q}, t) = \chi^{out}(\bar{Q}, t) + \chi^{in}(\bar{Q}, t) \quad (6)$$

to separate the components for the intramolecular (in) and intermolecular (out) contributions.

Developing the outer component results in:

$$\chi^{out}(\bar{Q}, t) = 4 b_c^2 j_0^2(Qb) I_d^{cm}(\bar{Q}, t) e^{-\gamma(t)Q^2}$$

where the distinct intermediate scattering function for the molecular centre of mass can be computed in the Sköld approximation to arrive at:

$$\chi^{out}(\bar{Q}, t) = 4 b_c^2 j_0^2(Qb) \{S^{cm}(Q) I_s^{cm}(Q/[S^{cm}(Q)]^{1/2}, t) - I_s^{cm}(\bar{Q}, t)\} \quad (7)$$

The intramolecular component is given by:

$$\chi^{in}(\bar{Q}, t) = v(\bar{Q}, t) I_s^{cm}(\bar{Q}, t) e^{-\gamma Q^2} \quad (8)$$

where $I_s^{cm}(\bar{Q}, t)$ is the intermediate scattering function due to the self-correlation of the centre of mass of the molecules, while $v(\bar{Q}, t)$ is due to the correlations of atoms within the same molecule, which includes the rotational motion around the centre of mass.

Finally, from Equations (5) to (8) is obtained:

$$S^{in}(Q, \omega) = \{S_{JJ'}(Q, \omega) \otimes S_s^{cm}(Q, \omega)\} e^{-\gamma Q^2}$$

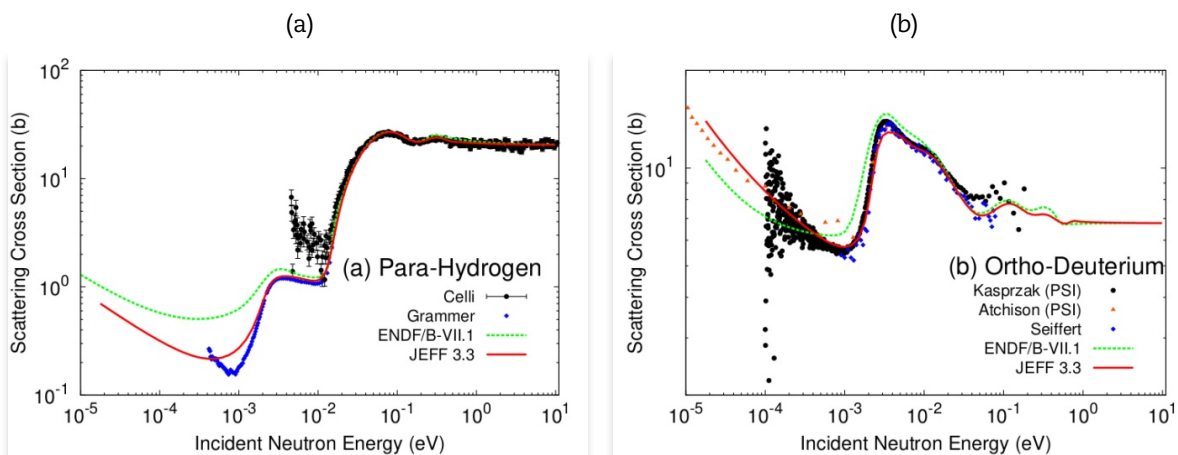
$$S^{out}(Q, \omega) = 4 b_c^2 j_0^2(Qb) \{S^{cm}(Q) S_s^{cm}(Q', \omega) - S_s^{cm}(Q, \omega)\} e^{-\gamma Q^2}$$

where $S_{JJ'}(Q, \omega)$ is the scattering law for the rotational motion of diatomic molecules developed by Young and Koppel (1964), $S^{cm}(Q)$ the structure factor of the centre of mass of the molecules, and $Q' = Q/[S^{cm}(Q)]^{1/2}$. These equations were implemented in a modified version of LEAPR, which is available from the authors at the website Github, <https://github.com/marquezj/NJOY2016/tree/H2D2> (Márquez Damián et al., 2018).

The models for liquid hydrogen and deuterium are completed with a representation of the dynamics and structure. The dynamics are modelled using the Egelstaff-Schofield diffusion model and continuous spectra that represent the collective dynamics of the molecule and were adapted from experimental data by Mukherjee et al. (1999). The structure factors were derived from experimental data by Zoppi (1996).

The models were validated using experimental data, and the calculations for para-hydrogen show a better agreement with total cross-sections measured by Celli et al. (1999) and Grammer et al. (2015) (see Figure 2.6a), whereas the calculations for ortho-deuterium show an improvement over previous models when compared with measurements performed at the Paul Scherer Institut by Kasprzak (2008) and Atchinson et al. (2005) (see Figure 2.6b).

Figure 2.6. **Total scattering cross-section of liquid para-hydrogen (left) and liquid ortho-deuterium (right) at 19 K**



Source: CAB.

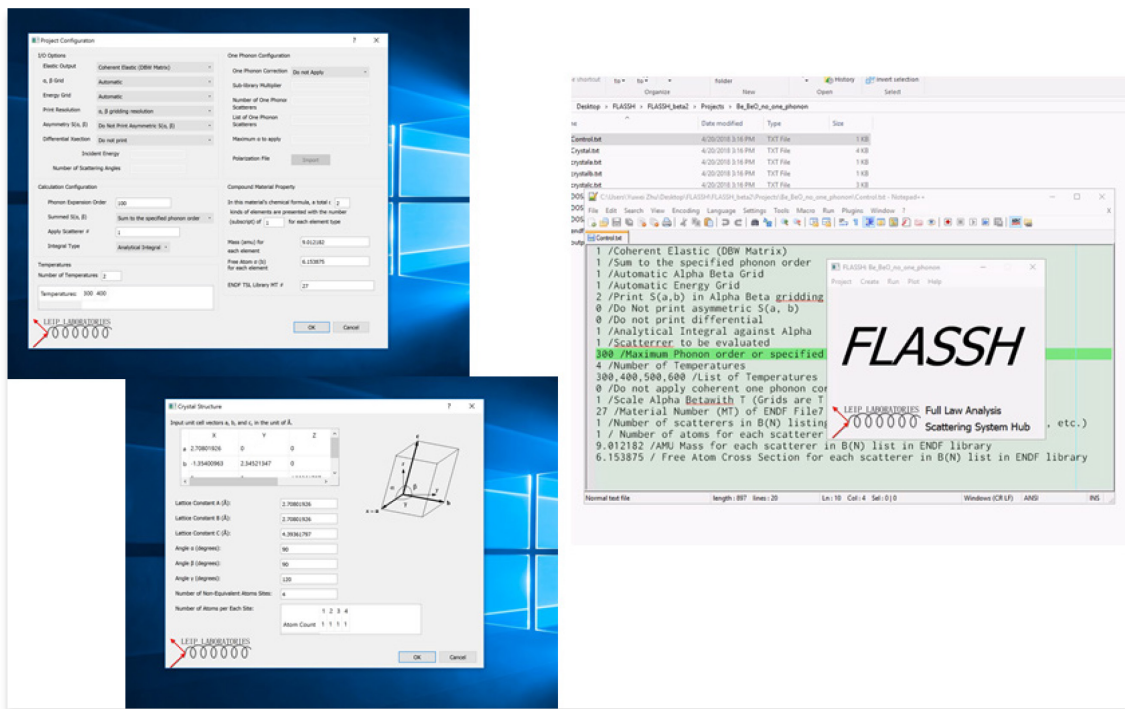
As shown in this section, the methodology applied by the Neutron Physics Department at CAB is a comprehensive approach that combines an extensive study of the material and the development of models that are implemented using open source tools that can be easily verified by third parties. The tools that are used in this process can be as simple as the Debye model used for modelling the relatively simple dynamics of neutron filters, or as complex as the combination of MD and experimental data (the “CAB model” [Márquez Damián et al., 2014]) used for the improvement of the evaluation of light and heavy water.

2.4. Future developments in TSL evaluation and processing

Developments at the NCSU

Beyond the discussion presented above, the development of TSL evaluation methods and tools focuses on the pursuit of a high-fidelity approach to support all levels of the analysis. In this case, tools have been under development for the past few years that include the FLASSH code of the NCSU (Zhu and Hawari, 2018). This code is capable of relaxing many of the approximations that were implemented in past tools such as GASKET and NJOY (Koppel et al., 1967; MacFarlane et al., 2017; MacFarlane, 1994). Figure 2.7 shows the computational graphical interface of FLASSH, which is used to simplify the user’s experience including the ability to diagnose input parameters. In addition, FLASSH is able to automate some tasks such as the optimum choice of certain input parameters, including the α and β grids. Table 2.1 summarises major aspects of FLASSH and compares it to LEAPR/NJOY. Figures 2.8 and 2.9 demonstrate FLASSH results for calculating the TSL of beryllium and aluminium with a comparison to LEAPR/NJOY and experimental data. However, it should be noted that FLASSH is developed to be backward compatible and, if needed, executable in a mode similar to LEAPR/NJOY.

Figure 2.7. A demonstration of the input and diagnostic interfaces of the FLASSH code



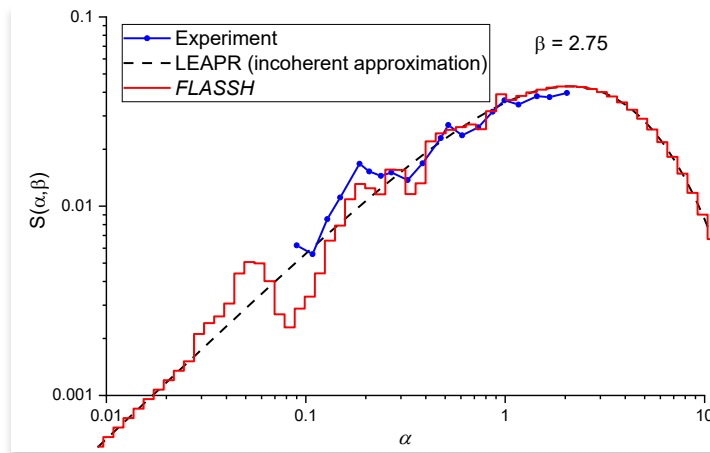
Source: NCSU.

Table 2.1. A comparison between the major features of NJOY and FLASSH for TSL evaluation

	NJOY (LEAPR and THERMR)	FLASSH
Remove incoherent approximation	No	Yes
Remove cubic approximation	No	Yes
Remove assumption of one atom per unit cell	No	Yes
Remove short collision time (SCT) approximation	No	Yes
Coherent elastic scattering	Approximate (hard coded for selected materials)	Exact formulation (any material based on user input)
Integral against α	Numerical	Analytical (optional numerical)
α, β grid	User input	Automatic (optional user input)
Parallel computing	No	Yes
Input syntax check	No	Yes
Graphical user interface	No	Yes

Source: NCSU.

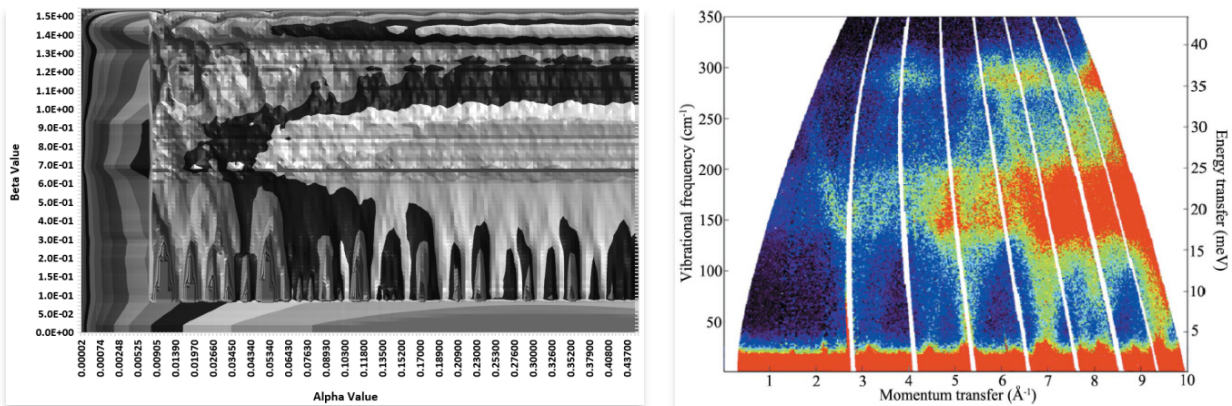
Figure 2.8. **A comparison of the measured TSL and the calculated TSL for beryllium metal**



Note: The calculation is performed using the LEAPR module of the NJOY code under the incoherent approximation [Equation (3) above] and the FLASSH code [with coherent inelastic (1-phonon) correction].

Source: NCSU.

Figure 2.9. **FLASSH analysis capturing coherent inelastic interference and showing a 3D view of the symmetric $S(\alpha, \beta)$ for aluminium above a minimum threshold for α and β**



Note: This example further illustrates the difference with respect to the incoherent approximation. The features are consistent with experimental measurements (Roach et al., 2013).

Source: Roach et al., 2013.

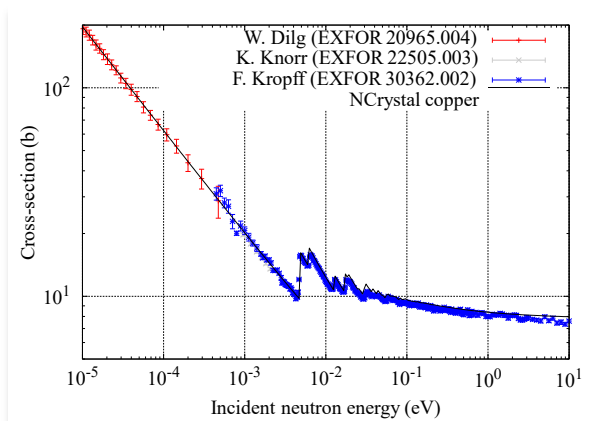
Developments at the European Spallation Source (ESS) and the Technical University of Denmark (DTU)

The European Spallation Source Detector Group and the Technical University of Denmark is working on a novel approach to the development and use of thermal scattering data. The project, called NCrystal (Kanaki et al., 2018), includes the development of a software toolkit and an associated material library (see Figure 2.7). The software toolkit is distributed as free software using the Apache 2.0 licence, which allows for third party codes to use and distribute it.

Instead of computing a TSL and formatting it into an evaluated nuclear data file, which is later processed and sampled in a Monte Carlo simulation, this software toolkit creates an object in memory, which is sampled using its own routines. This allows the Monte Carlo code to become independent from the physics development in thermal scattering and to easily extend the physics beyond the limits of the different library formats.

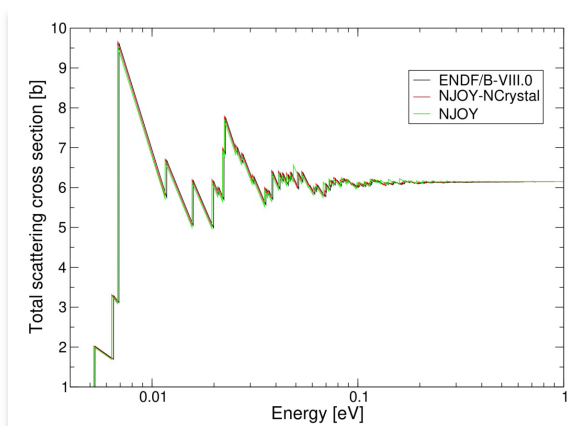
NCrystal started as a project to extend the treatment of scattering in crystals in the Monte Carlo code Geant4 (Agostinelli et al., 2003) using the extension NXSG4 (Kittelmann and Boin, 2015) and it is now a generic framework that can be used in a standalone manner or called from Geant4 or the neutron ray-trace simulation package McStas (Willendrup et al., 2004). NCrystal has also been linked to NJOY to provide the calculation of coherent elastic cross-sections for any crystalline structure (see Figure 2.8) without the use of proprietary or closed source software. NCrystal is now being extended to include the simulation of inelastic events using direct $S(\alpha, \beta)$ sampling (Cai et al., 2018).

Figure 2.10. **Total neutron cross-section for metallic copper computed with NCrystal, compared with experimental data from EXchange FORmat (EXFOR)**



Source: CAB.

Figure 2.11. **Calculation of the total cross-section of metallic beryllium using NJOY and NJOY-NCrystal compared with ENDF/B-VIII.0**



Source: CAB.

Developments at CAB

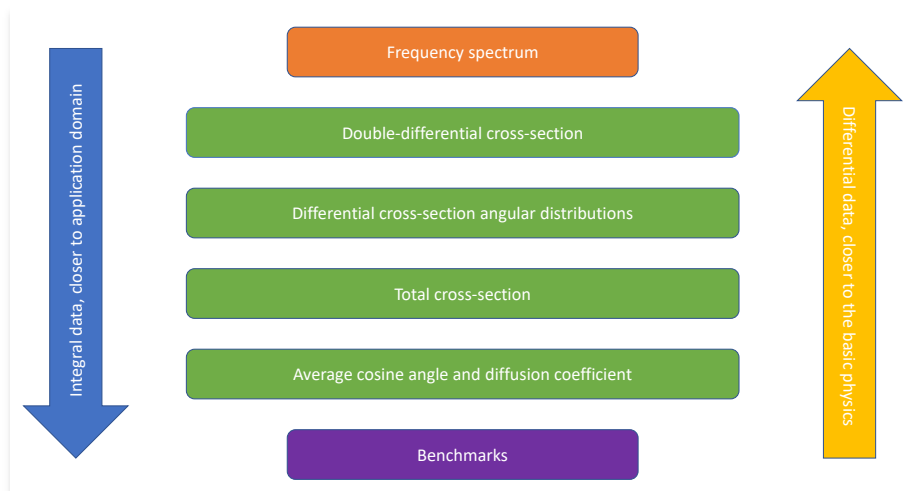
After the open source release of NJOY-2016, researchers at CAB have been contributing to the development and debugging of the LEAPR module. The patches required to compute and process the evaluations that were contributed to ENDF/B-VIII.0 have been transferred to the developing team and are now part of the official release of NJOY-2016. Aside from this, and by request of the user community, a set of interpolating routines has been developed to produce thermal scattering libraries of light and heavy water, on demand, at the required temperature by a non-expert user. These routines have been transferred to the International Atomic Energy Agency (IAEA) Nuclear Data Section and are currently hosted at the IAEA Nuclear Data Section website (IAEA, 2017).

Chapter 3. Experimental validation

The evaluation and validation of thermal scattering law (TSL) libraries can be supported by a measurement approach that holistically examines such libraries. The approach should recognise that the TSL is a material property and should account for the variation in neutron interactions as a function of the neutron energy (or wavelength). The following sections list the experimental measurements of interest that have been discussed during the mandate of the NEA Working Party on International Nuclear Data Evaluation Co-operation (WPEC)/Subgroup 42 (SG 42), but it should not be considered as an exhaustive list.

The validation can be performed at different levels, from microscopic material properties and differential measurements to integral measurements and benchmark calculations (see Figure 3.1). Validation at a microscopic and differential level is useful to verify the physics of the models, but not necessarily to test the effects that can be seen in neutron transport applications. Validation with integral quantities or benchmarks is closer to the application, but may suffer from compensation errors.

Figure 3.1. **Hierarchy of validation levels for thermal scattering libraries**



Source: CAB.

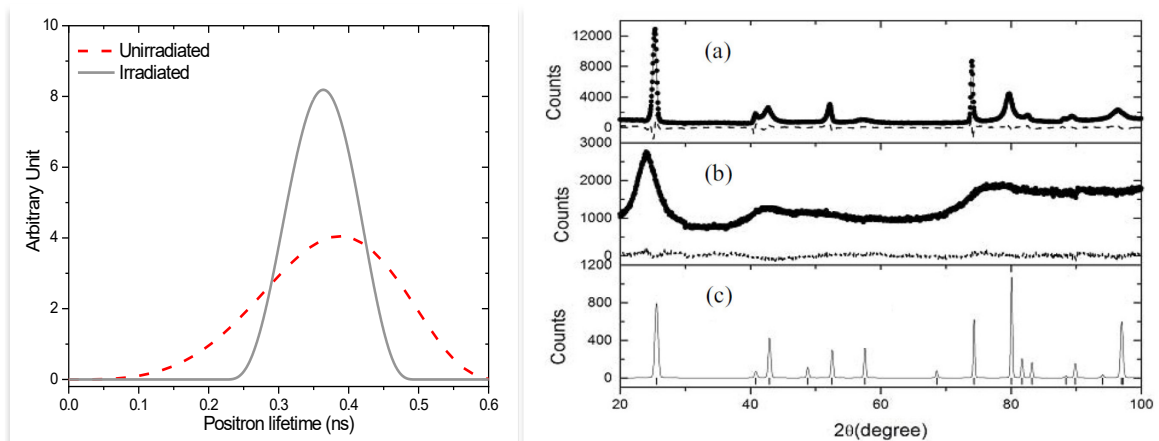
3.1. Experimental programme at North Carolina State University

Microscopic materials characterisation and measurements

The implementation of atomistic simulation methods to support TSL evaluation motivates the need for various experiments to probe the microstructure of the materials of interest and to measure thermo-physical properties. For that purpose, at the North Carolina State University (NCSU) PULSTAR reactor, techniques of neutron powder diffraction (NPD) and positron annihilation spectroscopy (PAS) were implemented and utilised to analyse “nuclear” graphite (Cai and Hawari, 2012; Liu and Hawari, 2014). In this case, PAS was

utilised to map the local electronic density of the material with the positron lifetime (i.e. time to annihilation) used as an indicator of the defect environment in the microstructure. In a complementary fashion, NPD was utilised to directly probe the atomic microstructure by using monochromatic neutron beams that are elastically scattered to form a sample. The collected diffraction patterns (and possibly extracted pair distribution functions) are used to infer details of the atomic microstructure. Figure 3.2 below shows the results of this analysis (Cai and Hawari, 2012; Liu and Hawari, 2014). NPD measurements observed the crystalline microstructure of unirradiated graphite (pattern a) but with distinct deviations from the ideal case (pattern c). In addition, for the irradiated graphite samples, the results showed a clear disruption in the crystalline nature of the microstructure (pattern b). The existences of intra-planar vacancies were deduced from the reduction in the basal plane dimensions that was observed in both cases. PAS analysis for unirradiated graphite samples resulted in a positron lifetime in the range of 0.2 to 0.5 nanoseconds. For irradiated graphite samples, the positron lifetime distribution narrowed by around 0.35 nanoseconds. These measurements indicated the existence of a porosity structure (e.g. vacancy clusters) that varies in size in both unirradiated and irradiated nuclear graphite. The information from both NPD and PAS measurements was used to formulate a model of “nuclear” graphite that is represented by a hexagonal crystalline structure with the addition of vacancies to account for density variations. Subsequently, this model was implemented in molecular dynamics (MD) simulations to produce first-of-a-kind “nuclear” graphite TSL libraries (Brown et al., 2018; Hawari and Gillette, 2014).

Figure 3.2. **PAS (left) and NPD (right) measurements performed at the NCSU PULSTAR reactor on unirradiated and irradiated “nuclear” graphite samples**



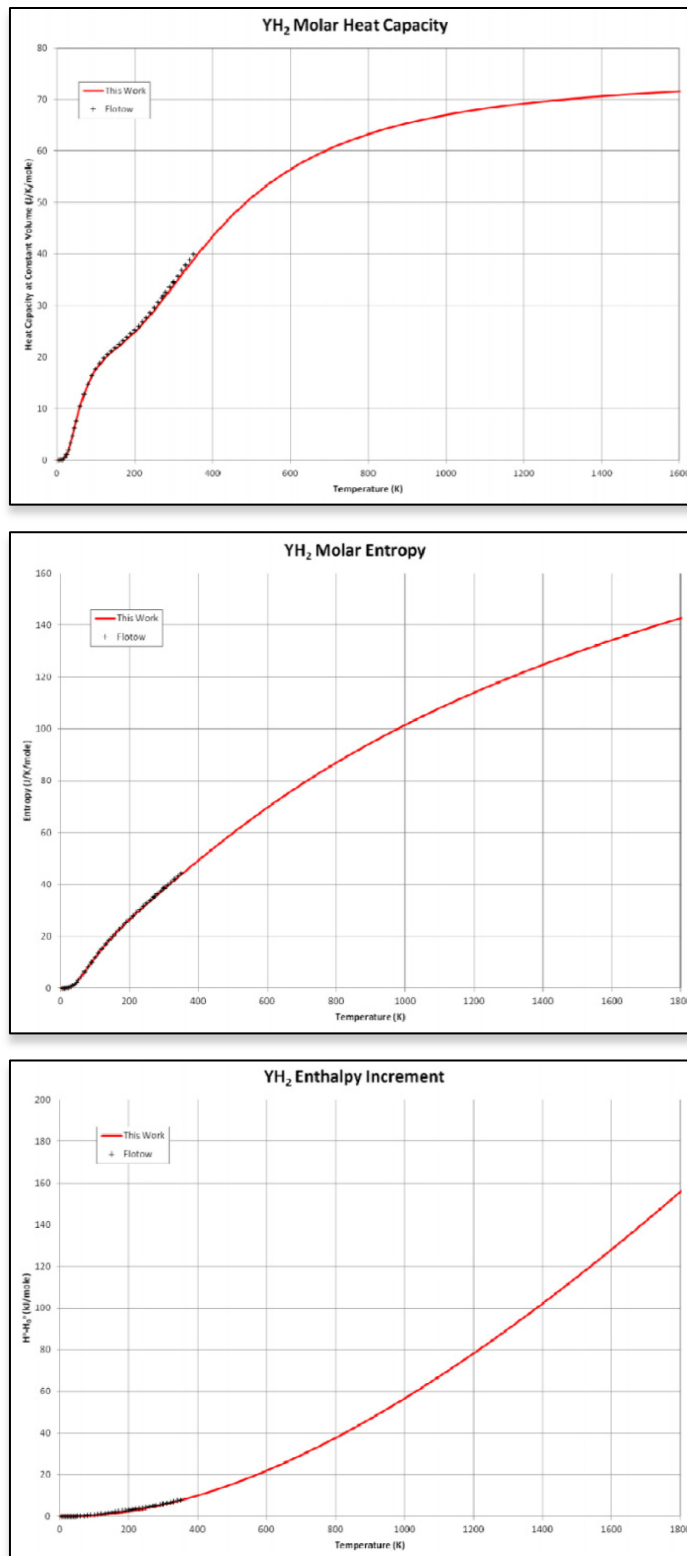
Source: Cai and Hawari, 2012.

Source: Liu and Hawari, 2014.

Note: In NPD, pattern a is for unirradiated graphite, pattern b is for irradiated graphite, and c is an ideal pattern generated using crystallographic calculations.

An additional example of using thermo-physical data to support the TSL evaluation process is shown in Figure 3.3 for the YH_2 evaluation performed by the US Naval Nuclear Laboratory. Thermodynamic properties of YH_2 as a function of the temperature can be well reproduced by calculations, ensuring reliable theoretical phonon density of states (DOS) for the LEAPR processing tool. However, experimental values available for validation steps usually cover small temperature ranges. In the case of YH_2 , the experimental validation is limited to $T < 350$ K. For reactor applications, higher temperatures of about 1 500 K are expected in the centre of the fuel pellets.

Figure 3.3. Examples of thermodynamic properties as a function of the temperature ($T < 350$ K) used to validate *ab initio* calculations for Yttrium hydride (YH_2)

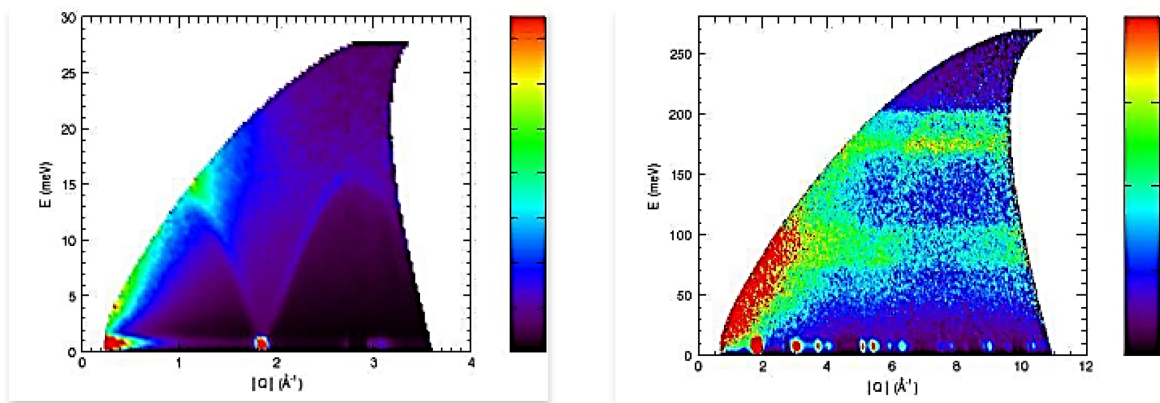


Source: National Naval Laboratory, United States.

Inelastic neutron scattering measurements

As part of the experimental programme at NCSU, inelastic neutron scattering (INS) measurements were performed on the same “nuclear” graphite samples described above. The measurements were performed at the SEQUOIA time-of-flight chopper spectrometer of Oak Ridge National Laboratory (ORNL) (Hawari et al., 2014). The measured data were used to produce $S(\alpha, \beta)$ and the generalised DOS (GDOS) for graphite. The measurements confirmed the general behaviour observed in the atomistic MD simulations of a “porous” graphite system (Hawari and Gillette, 2014), and this despite limitations related to instrument resolution and the limited coverage of α and β space. Figure 3.4 below shows the $G(Q, E)$ contours obtained from these measurements, which are used to extract the GDOS by integrating over Q . Figure 3.5 shows the resulting GDOS. In both figures, the results indicate a softening in the phonon spectrum where the regions related to low energy (and low momentum) transfers are enhanced. As shown in Figure 3.5, this clearly differs from the behaviour observed for the ideal phonon spectrum as calculated using *ab initio* atomistic simulations.

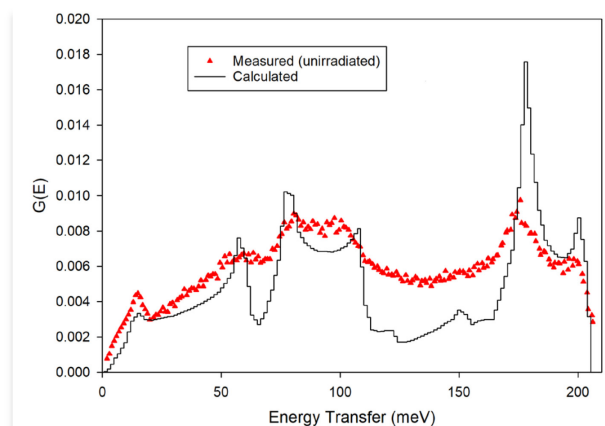
Figure 3.4. Measured $G(Q, E)$ contours for “nuclear” graphite



Note: The measurements were performed at the SEQUOIA time-of-flight spectrometer using 30 meV (left) and 280 meV (right) incoming neutron energies.

Source: Hawari et al., 2014.

Figure 3.5. Nuclear graphite measured and calculated (using *ab initio* atomistic simulations) GDOS



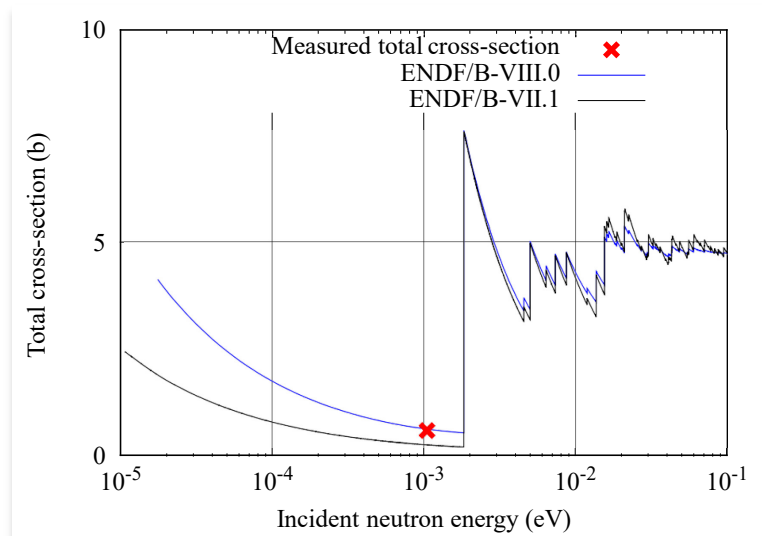
Note: The optical peaks around 180 and 200 meV are significantly reduced in the measured data in comparison to calculations. The measured lower energy regions are enhanced, including below 50 meV.

Source: NCSU.

Integral and semi-integral measurements

Total cross-section measurements using transmission experiments represent a class of integral measurements. For crystalline solids, measurements using neutrons with energy below the Bragg cut-off can provide data that directly probe the total inelastic scattering cross-section (Hawari et al., 2009). This type of measurement was performed for nuclear graphite and is shown in Figure 3.6 below. Clearly, the measurement shows excellent agreement with the Evaluated Nuclear Data File (ENDF)/B-VIII.0 evaluation that was based on the porous graphite model developed at NCSU. In addition, the measurement is consistent with previous measurements of this type that were also performed on nuclear graphite.

Figure 3.6. **The total cross-section of nuclear graphite measured using nine angstrom (1 meV) neutrons at the National Institute of Standards and Technology reactor**

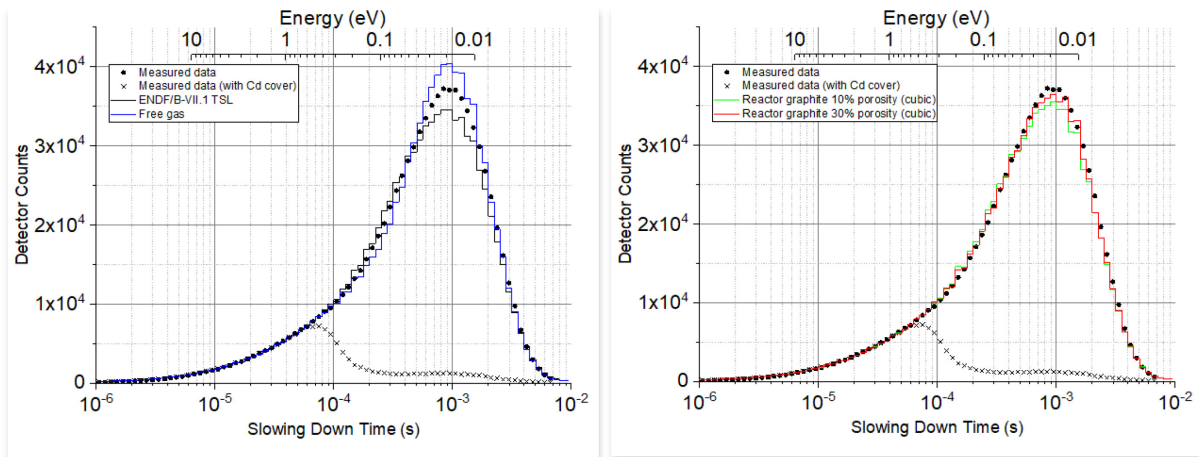


Note: The measured value is compared to the ENDF/B-VIII.0 nuclear graphite 30% porosity evaluation and the ENDF/B-VII.1 graphite evaluation.

Source: NCSU.

Semi-integral measurements have demonstrated utility in validating TSL evaluations (Hawari and Wehring, 2014). This includes the use of pulsed slowing-down-time (PSDT) experiments to benchmark TSL data. In particular, the PSDT method was successfully implemented to benchmark the TSL of graphite and to compare the response of detectors placed in the vicinity of a graphite pile to computational predictions using ENDF/B-VII.1 and ENDF/B-VIII.0 TSL libraries. In this case, the benchmark process benefits from two major characteristics of this approach: 1) the ability to quantitatively identify and isolate the portion of the detector response that is due to thermal neutrons; and 2) the ability to directly compare the experimental data to the computational results without resorting to model assumptions that may introduce interpretation biases. Figure 3.7 below shows a comparison of measurement and calculations in a graphite PSDT (Hawari et al., 2016).

Figure 3.7. **A comparison of the measured and predicted detector response in the NCSU PSDT experiment performed in a graphite pile at the Oak Ridge Electron Linear Accelerator (ORELA) facility**



Note: The left plot shows the predictions of the ENDF/B-VII.1 graphite TSL library. The right plot shows the predictions of the ENDF/B-VIII.0 nuclear/reactor graphite TSL libraries with a porosity of 10% (tsl-reactor-graphite-10P.endf) and a porosity of 30% (tsl-reactor-graphite-30P.endf). The measured data with a cadmium cover shows that at approximately 100 μ s slowing down time (i.e. time after the pulse) the neutron average energy drops below 0.5 eV. Source: NCSU.

The outcome of the NCSU measurement programme to study nuclear graphite demonstrated that while each technique probes different aspects relevant to the thermal scattering phenomenon, the conclusions of all techniques (for a given material) should converge to support the validation of the material's TSL. Clearly, this approach can be used to support TSL evaluations for other materials.

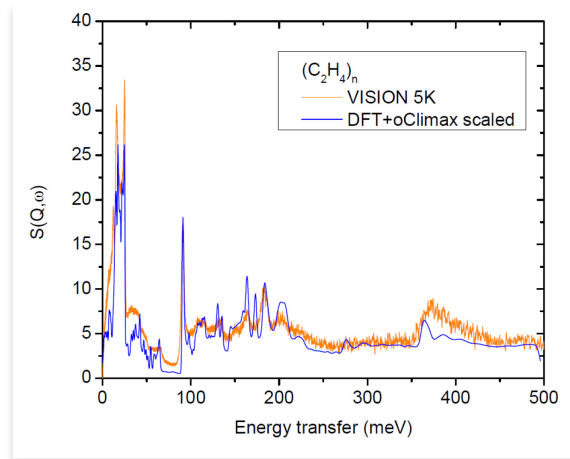
3.2. Experimental programmes at Spallation Neutron Source (ORNL, United States)

In terms of inelastic experiments, the recent efforts by the Rensselaer Polytechnic Institute (RPI) Nuclear Data Group, outlined in the article entitled “Thermal Scattering Law of C_2H_4n : Integrating Experimental Data with DFT Calculations” (Ramić et al., 2018), have identified two sets of neutron spectrometers to be used for the determination of TSL:

- direct geometry neutron spectrometers, such as ARCS and SEQUOIA spectrometers at the Spallation Neutron Source (SNS, ORNL) that provide double-differential scattering cross-section (DDSCS) measurements at any desired temperature starting at 5 K, and any neutron incident energy;
- indirect geometry neutron spectrometers, such as VISION at SNS ORNL, where the measured quantity is $S(Q, \omega)$ in the desired continuous energy range (up to 500 meV). The data from VISION spectrometer, because of the design of the spectrometer (“white” beam incident energy spectra, Q -dependence parallel to c -axis of the sample and the momentum transfer proportionality to the energy transfer), was more suitable to transformation of $S(Q, \omega)$ to GDOS than the ARCS data (see Figure 3.8).

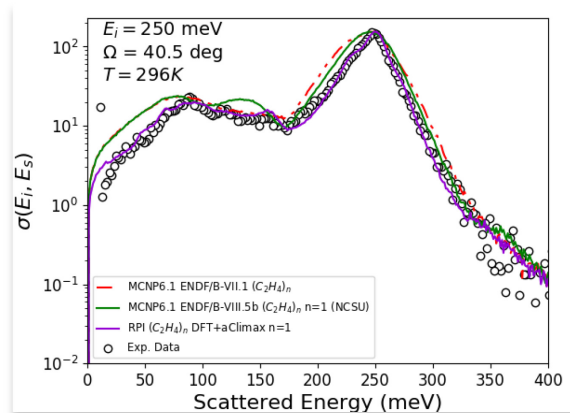
The experimental DDSCS data, as seen in Figure 3.9 for polyethylene, is used to validate how well the newly created TSLs calculate the DDSCS. In addition to polyethylene, inelastic neutron scattering measurements on quartz, lucite, teflon, concrete and Ice I_h have also been performed by the RPI Nuclear Data Group (Ramić, 2018).

Figure 3.8. **Comparison of VISION $S(Q, \omega)$ and $S(Q, \omega)$ calculated using CASTEP and oClimax after the locations of the peaks have been adjusted to match the experimental data**



Source: RPI.

Figure 3.9. **Comparison of the experimental DDSGS from ARCS at 250 meV incident neutron energy and DDSGS calculated using oClimax derived phonon spectrum with NJOY-2016**



Source: NCSU.

3.3. Experimental programmes at the Institut Laue-Langevin (Grenoble, France)

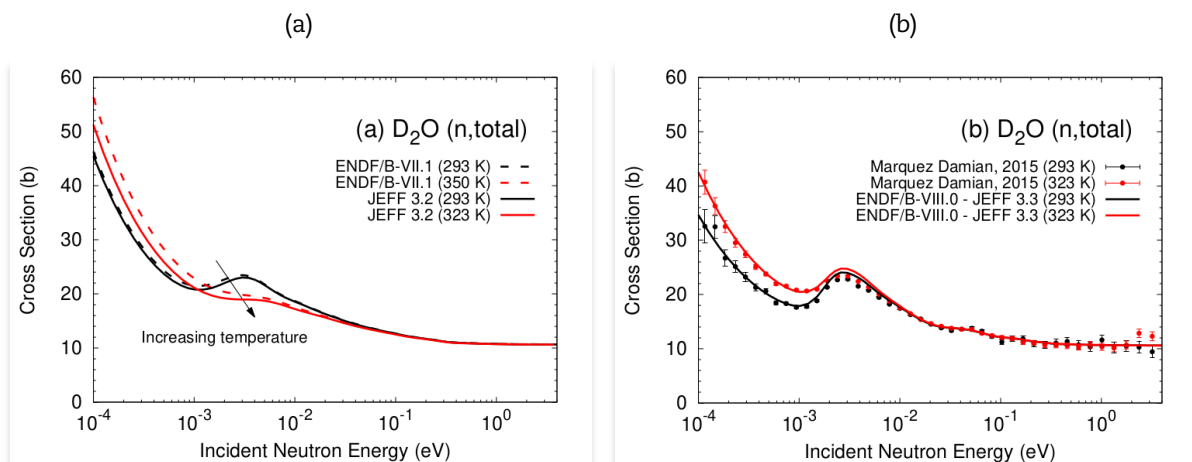
Inelastic neutron scattering experiments were carried out in the framework of an experimental project started mid-2014 at the Institut Laue-Langevin (ILL), for which the goal was to measure double-differential cross-sections and to produce dynamic structure factor $S(\alpha, \beta)$. Experimental results were already obtained for light water, heavy water and uranium dioxide as a function of temperature (and pressure for water). Three time-of-flight spectrometers were used, namely IN4, IN5 and IN6. The flight-length varies from 2 m to 5 m. The obtained data were first used to validate TSL available in the neutron libraries. In that case, experimental results are compared with Monte Carlo simulations (such as TRIPOLI4). For water, TSL files were generated with the LEAPR module of NJOY via the experimental phonon DOS provided by the IN4 spectrometer.

3.4. Experimental Programme for Centro Atómico Bariloche and collaborators

Temperature dependence in heavy water

As part of collaboration efforts within subgroup members, an anomalous behaviour of the temperature dependence of the total cross-section of heavy water in the models used in ENDF/B-VII.1 and Joint Evaluated Fission and Fusion File (JEFF)-3.2 was initially identified by Canadian Nuclear Laboratories (see Figure 3.10a). The problem was studied by members of the Neutron Physics Department at Centro Atómico Bariloche (CAB), and it was recognised that this anomalous behaviour was not observed in the new models. To settle the issue, a neutron transmission experiment was proposed and carried out at the Low Energy Neutron Source of Indiana University (Márquez Damián et al., 2015). The experimental results do not show this behaviour and served as validation of the CAB model for heavy water (see Figure 3.10b).

Figure 3.10. Temperature dependence of the total thermal neutron cross-section of heavy water as a function of energy



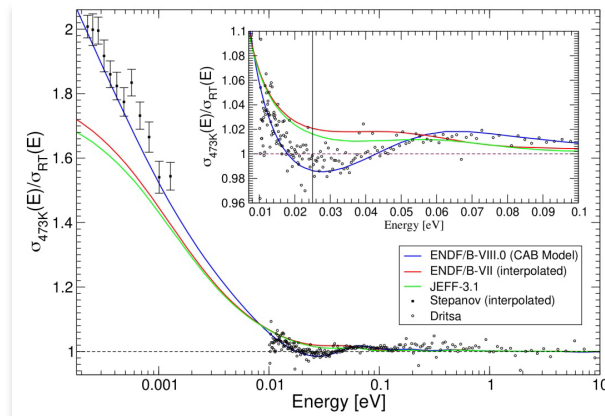
Note: (a) Anomalous behaviour predicted by the model used in ENDF/B-VII.1 and JEFF-3.2. (b) Calculations used the CAB model (incorporated in ENDF/B-VIII.0 and JEFF-3.3), compared with transmission experiments performed at Indiana University.

Source: Márquez Damián et al., 2015.

Temperature dependence in light water

When the CAB model was first introduced, it was observed by researchers from the French Alternative Energies and Atomic Energy Commission (CEA) in Cadarache that the shift in the rotational spectrum caused a slight reduction of the predicted total neutron cross-section when the temperature was raised from 20 to 200°C. This effect was indeed confirmed with data from the Demokritos reactor in Greece, where it was observed experimentally in the 1960s by Dritsa and Kostikas (1967) (see Figure 3.11). The temperature behaviour of the new models was also validated using data from Stepanov et al. (1974).

Figure 3.11. **Temperature dependence of the total thermal neutron cross-section of light water as a function of energy, shown as the ratio of the total cross-section at 473 and 293 K**

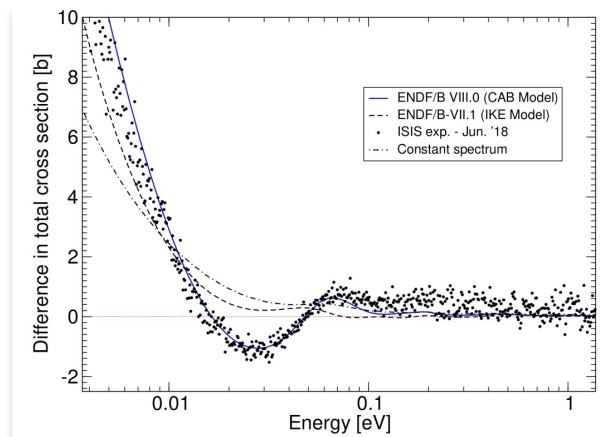


Note: The data from Stepanov was interpolated from datasets at 453 and 488 K.
Source: CAB.

Later, researchers from the US Naval Nuclear Laboratory raised the question of whether this effect was also observable at lower temperatures, which could have an impact in proprietary benchmarks based on experiments in the Neptune zero power reactor (Walley et al., 2016). In order to test this possibility, a transmission experiment was carried out at the VESUVIO spectrometer in the ISIS Neutron Source in the United Kingdom. The experimental results confirm the predictions of the CAB model (see Figure 3.12).

These new measurements fill a gap in the availability of experimental, total cross-section data for light water (see Figure 3.13). At the same time, there is a significant region of the energy/temperature map that has yet to be measured and would provide an important tool for the validation of light water thermal scattering models.

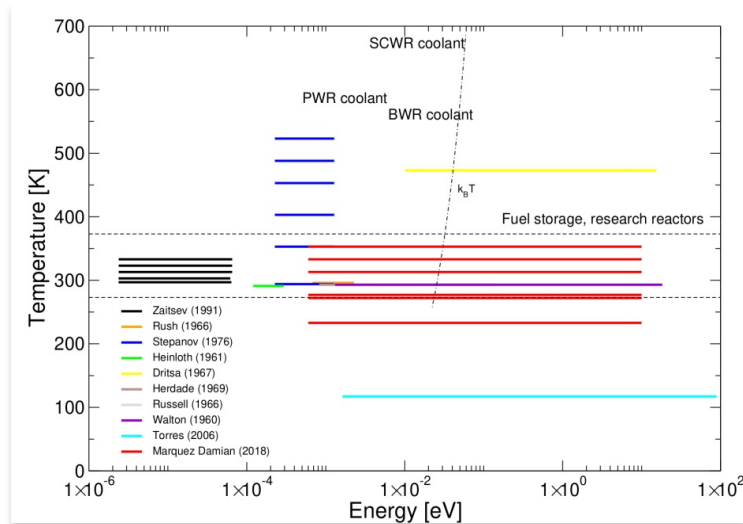
Figure 3.12. **Temperature dependence of the total thermal neutron cross-section of light water as a function of energy, shown as the difference of the total cross-section at 353 and 283 K**



Note: The preliminary results from the experiment are compared with calculations performed using ENDF/B-VIII.0 (CAB model), ENDF/B-VII.1 (IKE Model) and a fictitious evaluation using the room temperature frequency spectrum of ENDF/B-VIII.0 for all temperatures.

Source: CAB.

Figure 3.13. **Experimental total neutron cross-section data sets for light water measured at different temperatures**



Note: The red lines shown are the measurements performed at VESUVIO in June 2018.
Source: CAB.

Compilation of thermal scattering data

In November 2015, the International Atomic Energy Agency (IAEA) Nuclear Data Section held a consultant's meeting on "Compilation of Thermal Neutron Scattering Data for Experimental Nuclear Reaction Data Library" (Márquez Damián and Semkova, 2015). As a result of this meeting, it was recommended to include thermal scattering reaction data in EXchange FORmat (EXFOR) and to set up a separate database for experimental and derived data that helps the process of TSL evaluation. This database was set up at the IAEA Nuclear Data Section website by Semkova (IAEA) and Márquez Damián (CAB) and can be accessed here (Márquez Damián and Semkova, 2015).

Experimental data on cryogenic moderators

As part of the contribution of Argentina to the IAEA Coordinated Research Project "Advanced Moderators for Intense Cold Neutron Beams in Materials Research", the Nuclear Data Group at CAB performed transmission experiments at the VESUVIO spectrometer of the ISIS Neutron Source at the Rutherford Appleton Laboratory, United Kingdom, to measure the total cross-section of liquid and solid triphenylmethane and liquid ethane.

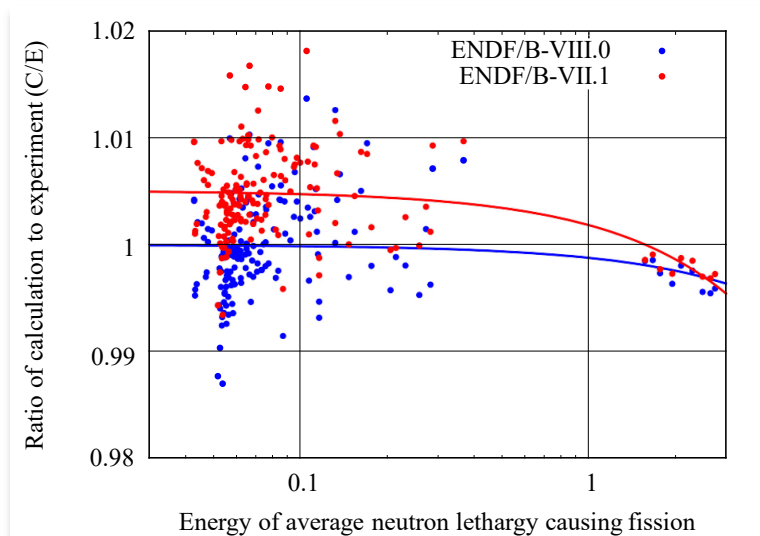
Triphenylmethane is an aromatic hydrocarbon proposed by Los Alamos National Laboratory (Hügler et al., 2014) as an alternative material for cold neutron sources at high-intensity facilities, because of its high-radiation stability. On the other hand, liquid ethane was proposed by CAB as a replacement of liquid methane in intermediate energy cold neutron sources, for which its wide temperature range in liquid phase and high proton density makes it a suitable candidate. These materials were studied and preliminary results (Cantargi et al., 2017) have suggested that more experimental data were necessary to validate the scattering.

3.5. Integral experiments

A large variety of integral data can be used to validate TSL evaluations. Unfortunately, many of them are also sensitive to other nuclear data. For example, compensating effects in the International Criticality Safety Benchmark Evaluation Project (ICSBEP) benchmarks are often subject to discussion. Integral benchmarks available in this database were designed for criticality and safety applications, in which actinides cross-sections, neutron multiplicities and prompt neutron fission spectra play a significant role. In these cases, the impact of TSL has to be assessed for the evaluated nuclear data library as a whole. For example, the combination of new evaluations for ^{239}Pu , ^{16}O from the Collaborative International Evaluated Library Organisation Pilot (CIELO) project and the new evaluation for the TSL of light water have allowed ENDF/B-VIII.0 to resolve a long-standing bias on the calculation of plutonium solution benchmarks (see Figure 3.14). However, it should be noted that some series of ICSBEP benchmarks are adequate for quantifying TSL impacts on k_{eff} values as a function of the spectrum hardness and when material under investigation is used as reflector.

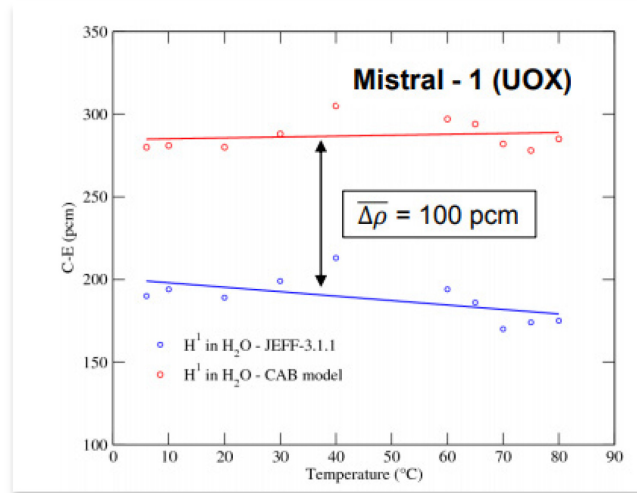
Similar difficulties arise when mock-up experiments for reactor applications are used for testing the performances of new TSL. Such issues were investigated with temperature-dependent integral experiments carried out at the zero power reactor EOLE (CEA Cadarache, France). Results obtained for light water are reported in Santamarina, 1989; Yamamoto et al., 1997; and Fougeras et al., 1999. The MISTRAL-1,2,3 programmes were designed to investigate reactivity temperature coefficients for uranium oxide (UOX) and mixed oxide (MOX) cores from 6°C to 80°C (step of 5°C). Experiments were first interpreted with the Monte Carlo code TRIPOLI-4 by using the JEFF-3.1.1 library. Then, TSLs of H in H_2O were replaced by those of ENDF/B-VII.1 and ENDF/B-VIII.0. Figure 3.15 compares the C-E results obtained with the TSL from JEFF-3.1.1 and ENDF/B-VIII.0, called the CAB model. The decreasing trend with the temperature observed with JEFF-3.1.1 vanishes when the TSL from ENDF/B-VIII.0 is used (Scotta et al., 2016).

Figure 3.14. **Multiplication factor of ICSBEP plutonium solution benchmarks as a function of the energy of average neutron lethargy causing fission (EALF) calculated using ENDF/B-VII.1 and ENDF/B-VIII.0**



Source: Brown et al., 2018.

Figure 3.15. **Differences between calculated (C) and experimental (E) reactivity obtained as a function of the temperature in the framework of the MISTRAL-1 programme carried out in the EOLE facility (CEA Cadarache)**



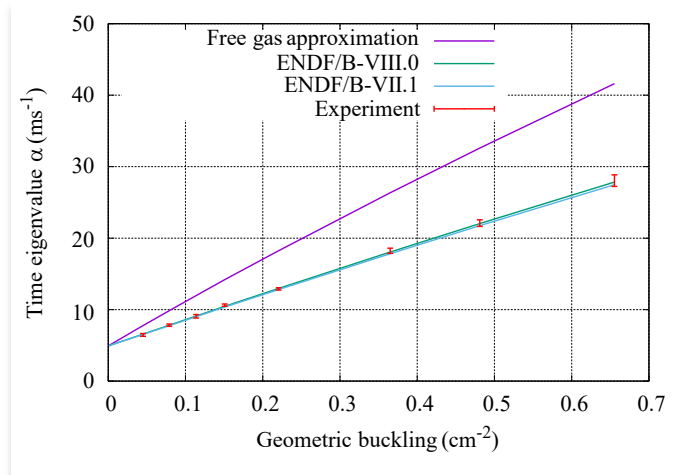
Source: CEA.

Alternative integral benchmarks for validating TSL were discussed on the basis of past pulsed neutron die away (PNDA) experiments carried out at Lawrence Livermore National Laboratory (LLNL) on ice, liquid water and other materials. From the obtained results, it is recommended that PNDA diffusion benchmarks be developed as an inexpensive and more sensitive method of validating the physics of TSL evaluations. Advantages of PNDA diffusion benchmarks include:

- the only reactions neutrons undertake are thermal scattering, absorption and leakage;
- in a simulation, there is no concern about nuclear data uncertainties from other materials;
- models are geometrically simple and the only material present is the material being tested;
- eigenvalue sensitivity to thermal scattering is a strong function of geometric buckling and can be controlled by sample size;
- absorption dominates in large samples, and thermal scattering dominates in small samples;
- samples can be easily heated or cooled to study thermal scattering temperature dependence;
- experiments require much less material than critical benchmarks and are much less expensive.

Figure 3.16 below shows PNDA results as calculated by the US National Nuclear Laboratory (NNL) for light water using the MC21 code with comparison to experiments. The TSL of hydrogen in light water with the new evaluation distinctly improves agreement with experiment, in comparison to simulations using free atom cross-sections or alternative TSL evaluations for hydrogen.

Figure 3.16. **Thermal flux time decay eigenvalues vs. buckling for liquid water spheres with selected thermal neutron scattering kernels**



Source: Experimental data from Nassar and Murphy, Nuclear Science and Engineering, Vol. 35 (1969).

3.6. Facilities for TSL experiments and capability gaps

Microscopic data presented during the SG 42 meetings mainly come from instruments available at the SNS (ORNL), ILL and the Low Energy Neutron Source (LENS, Indiana University, United States). These facilities can provide total and double-differential scattering cross-sections within neutron energy ranges that vary between the instruments. For the total cross-sections, the LENS facility covers a wide energy range, from 0.1 meV to 1 eV, and energies below 0.1 meV can be achieved, for example, at the cold neutron source of ILL. In comparison, only a few wavelengths are available at the inelastic spectrometers (IN4, IN5 and IN6) of ILL, corresponding to neutron energies ranging from 1 meV to 100 meV.

For the experimental conditions, the facilities offer possibilities to measure data as a function of (P,T), from cold conditions up to hot zero power operating conditions (P<200 bar, T<2000 K). For the inelastic instruments, the time-resolution of the instruments is a key parameter. Experimental results presented during the meetings show that the time-resolution at SNS (ARCS and SEQUOIA) and ILL (IN5) is good enough to validate new TSL. However, improvements would be needed, especially for an accurate measurement of high-energy vibration modes, such as bending and stretching modes in the water molecule.

Among the low-energy physics instruments, the VISION detector at SNS is quite unique because it allows for the measurement of DOS with a high resolution over a large q range (up to 1 000 meV energy transfer). As explained in Section 2.3, the oClimax software can be used to extract an experimental phonon spectrum free from multiple scattering and resolution broadening from the VISION data.

According to discussions, low-energy instruments and data analysis tools available in the different institutes are mature for providing high-quality data for evaluation and validation purposes.

Chapter 4. Thermal scattering law data format and uncertainty issues

Currently, evaluations of thermal neutron scattering are presented in the Evaluated Nuclear Data File (ENDF)-6 format (File MF=7). In this format, File 7 includes a MF=7 MT=2 section that tabulates the coherent elastic cross-sections and a MF=7 MT=4 section that tabulates the thermal scattering law (TSL), $S(\alpha, \beta)$. Typically, File 7 tabulates the symmetric form of $S(\alpha, \beta)$. In addition, the TSL is tabulated for a given temperature and over defined α and β grids. The details of the format and content of a TSL File 7 are given in “ENDF-6 Formats Manual, Data Formats and Procedures for the Evaluated Nuclear Data Files ENDF/B-VI and ENDF/B-VII” (CSEWG, 2010).

4.1. Modern TSL library format

During the past decade, a new format for nuclear data files was established (Mattoon et al., 2012). This is represented by the Generalised Nuclear Data Structure (GNDS) format. Within the GNDS format, several structures were considered for TSL files. These structures accounted for the developments in TSL analysis discussed in the previous sections, including the relaxation of approximations and the ability to generate more complete and accurate TSL data. Quantitatively, and using the TSL formulation as guidance, three potential options emerge for the GNDS TSL format that have data blocks reflecting the double-differential formulations presented in Table 4.1.

$$\frac{d^2\sigma}{d\Omega dE'} = \frac{1}{4\pi k_B T} \sqrt{\frac{E'}{E}} [\sigma_{coh} S + \sigma_{inc} S_s] \quad (\text{option 1})$$

where all the symbols have their standard meaning. Methods such as molecular dynamics (MD) analysis can calculate S and S_s . Assuming utilisation of the phonon expansion approach and noting that $S = S_s + S_d$, the above can be written as:

$$\frac{d^2\sigma}{d\Omega dE'} = \frac{1}{4\pi k_B T} \sqrt{\frac{E'}{E}} \left[\sigma_{coh} ({}^1S_s + {}^1S_d) + \sigma_{inc} {}^1S_s + (\sigma_{coh} + \sigma_{inc}) \sum_{p=2}^p S_s \right] \quad (\text{option 2})$$

The phonon expansion order is indicated as p . Alternatively, the above equation can be written as:

$$\frac{d^2\sigma}{d\Omega dE'} = \frac{1}{4\pi k_B T} \sqrt{\frac{E'}{E}} [(\sigma_{coh} + \sigma_{inc}) S_s + \sigma_{coh} {}^1S_d] \quad (\text{option 3})$$

Typically, the equations for both options 2 and 3 assume the utilisation of methods that apply the phonon expansion approach. The figures below (4.1-4.3) illustrate potential TSL formats using uranium nitride (UN) as the evaluated material. It should also be noted that the GNDS format can now include the incoherent and coherent elastic components simultaneously in the same TSL library (e.g. as would be needed for UN). Previously, this was not allowed when using the traditional ENDF-6 File 7 format (CSEWG, 2010).

The option 3 equation can be equivalently expressed as:

$$\frac{d^2\sigma}{d\Omega dE'} = \frac{(\sigma_{coh} + \sigma_{inc})}{4\pi k_B T} \sqrt{\frac{E'}{E}} \left[S_s + \frac{\sigma_{coh}}{(\sigma_{coh} + \sigma_{inc})} {}^1S_d \right],$$

where this form allows the option of a TSL format that stores S_s and $\left[\frac{\sigma_{coh}}{(\sigma_{coh} + \sigma_{inc})} {}^1S_d \right]$.

Table 4.1. New and updated TSL libraries in the ENDF/B-VIII.0 and JEFF-3.3 releases contributed by NCSU, CAB, CNL and BAPL

Material	Evaluation basis	Institution	Library
Beryllium metal	DFT/LD	NCSU	ENDF/B-VIII.0
Beryllium oxide (beryllium)	DFT/LD	NCSU	ENDF/B-VIII.0
Beryllium oxide (oxygen)	DFT/LD	NCSU	ENDF/B-VIII.0
Polymethyl methacrylate (Lucite)	MD	NCSU	ENDF/B-VIII.0
Polyethylene (hydrogen)	MD	NCSU	ENDF/B-VIII.0
Crystalline graphite	MD	NCSU	ENDF/B-VIII.0
Reactor graphite (10% porosity)	MD	NCSU	ENDF/B-VIII.0
Reactor graphite (30% porosity)	MD	NCSU	ENDF/B-VIII.0
Silicon carbide (silicon)	DFT/LD	NCSU	ENDF/B-VIII.0
Silicon carbide (carbon)	DFT/LD	NCSU	ENDF/B-VIII.0
Silicon dioxide (alpha phase)	DFT/LD	NCSU	ENDF/B-VIII.0
Silicon dioxide (beta phase)	DFT/LD	NCSU	ENDF/B-VIII.0
Uranium dioxide (oxygen)	DFT/LD	NCSU	ENDF/B-VIII.0
Uranium dioxide (uranium)	DFT/LD	NCSU	ENDF/B-VIII.0
Uranium nitride (nitrogen)	DFT/LD	NCSU	ENDF/B-VIII.0
Uranium nitride (uranium)	DFT/LD	NCSU	ENDF/B-VIII.0
Light water ice I _h (hydrogen)	DFT/LD	BAPL	ENDF/B-VIII.0
Light water ice I _h (oxygen)	DFT/LD	BAPL	ENDF/B-VIII.0
Yttrium hydride (hydrogen)	DFT/LD	BAPL	ENDF/B-VIII.0
Yttrium hydride (yttrium)	DFT/LD	BAPL	ENDF/B-VIII.0
Light water (hydrogen)	Exp. data/MD	CAB, CNL	ENDF/B-VIII.0
Heavy water (deuterium)	Exp. data/MD	CAB, CNL	ENDF/B-VIII.0, JEFF-3.3
Heavy water (oxygen)	Exp. data/MD	CAB, CNL	ENDF/B-VIII.0, JEFF-3.3
Sapphire (aluminium)	Exp. data/Debye model	CAB	JEFF-3.3
Sapphire (oxygen)	Exp. data/Debye model	CAB	JEFF-3.3
Ortho-deuterium	Exp. data	CAB	JEFF-3.3
Para-deuterium	Exp. data	CAB	JEFF-3.3
Light water ice I _h (hydrogen)	Exp. data	CAB	JEFF-3.3
Mesitylene Ph. II (hydrogen)	Exp. data	CAB	JEFF-3.3
Ortho-hydrogen	Exp. data	CAB	JEFF-3.3
Para-hydrogen	Exp. data	CAB	JEFF-3.3
Toluene Ph. II (hydrogen)	Exp. data	CAB	JEFF-3.3
Silicon	Exp. data/Debye model	CAB	JEFF-3.3

Notes: NCSU – North Carolina State University; CAB – Centro Atómico Bariloche; CNL – Canadian Nuclear Laboratories; BAPL – Bettis Atomic Power Laboratory; DFT – density functional theory; LD – Lattice dynamics; MD – Molecular dynamics; ENDF – Evaluated Nuclear Data File; JEFF – Joint Evaluated Fission and Fusion File.

Figure 4.1. An example of “Option 1” for the GNDS format of TSL data

```

1
2
3 <thermalScattering
4   material="U (UN) "
5   MAT="72">
6   <documentations>
7     <documentation style="endfDoc">
8       <documentation name="endfDoc"><![CDATA[
9         U (UN)   LEIP LAB   EVAL-SEP17 J.L. Wormald, A.I. Hawari
10        NDS 148, 1 (2018)   DIST-FEB18
11        ----ENDF/B-VIII.0   MATERIAL 72
12        -----THERMAL NEUTRON SCATTERING DATA
13        -----ENDF-6 FORMAT
14        Temperatures = 296 400 500 600 700 800 1000 1200 K
15
16        Background
17        -----
18        ...
19      ]]>
20    </documentation>
21  </documentations>
22  <scatteringAtoms>
23    <scatteringAtom label="0" numberPerMolecule="1">
24      <mass value="236.0058" unit="amu"/>
25      <CoherentBoundCrossSection value="9.283302" unit="b"/>
26      <IncoherentBoundCrossSection value="9.283302" unit="b"/>
27      <e_critical value="197.6285" unit="eV"/>
28      <e_max value="5.000001" unit="eV"/>
29      <coherentElastic>
30        <S_table>...</S_table>
31      </coherentElastic>
32      <IncoherentElastic calculatedAtThermal="true">
33        <DebyeWaller>...</DebyeWaller>
34      </IncoherentElastic>
35      <IncoherentInelastic>
36        <T_effective>
37          <axes>
38            <axis index="1" label="temperature" unit="K"/>
39            <axis index="0" label="t_effective" unit="K"/></axes>
40          <values>296 306.097 4e2 407.5307 5e2 ... 1200 1202.533</values>
41        </T_effective>
42        <Ss_alpha_beta>...</Ss_alpha_beta>
43      </IncoherentInelastic>
44      <Inelastic>
45        <S_alpha_beta>...</S_alpha_beta>
46      </Inelastic>
47    </scatteringAtom>
48  </scatteringAtoms>
49 </thermalScattering>
50

```

Note: This option is most general and takes advantage of the ability of modern techniques (e.g. classical molecular dynamics [MD] or *ab initio* MD) to calculate the content of its data blocks (i.e. S and S_s).

Figure 4.2. An example of “Option 2” for the GNDS format of TSL data

```

1
2
3 <thermalScattering
4   material="U (UN) "
5   MAT="72">
6 <documentations>
7   <documentation style="endfDoc">
8     <documentation name="endfDoc"><![CDATA[
9       U(UN)      LEIP LAB      EVAL-SEP17 J.L. Wormald, A.I. Hawari
10      NDS 148, 1 (2018)      DIST-FEB18
11      ----ENDF/B-VIII.0      MATERIAL 72
12      ----THERMAL NEUTRON SCATTERING DATA
13      ----ENDF-6 FORMAT
14      Temperatures = 296 400 500 600 700 800 1000 1200 K
15
16      Background
17      -----
18      ...
19      ]]>
20   </documentation>
21 </documentations>
22 <scatteringAtoms>
23   <scatteringAtom label="0" numberPerMolecule="1">
24     <mass value="236.0058" unit="amu"/>
25     <CoherentBoundCrossSection value="9.283302" unit="b"/>
26     <IncoherentBoundCrossSection value="9.283302" unit="b"/>
27     <e_critical value="197.6285" unit="eV"/>
28     <e_max value="5.000001" unit="eV"/>
29     <coherentElastic>
30       <S_table>...</S_table>
31     </coherentElastic>
32     <IncoherentElastic calculatedAtThermal="true">
33       <DebyeWaller>...</DebyeWaller>
34     </IncoherentElastic>
35     <IncoherentInelastic>
36       <T_effective>
37         <axes>
38           <axis index="1" label="temperature" unit="K"/>
39           <axis index="0" label="t_effective" unit="K"/></axes>
40         <values>296 306.097 4e2 407.5307 5e2 ... 1200 1202.533</values>
41       </T_effective>
42       <Ss_alpha_beta>...</Ss_alpha_beta>
43       <Ss1_alpha_beta>...</Ss1_alpha_beta>
44     </IncoherentInelastic>
45     <CoherentInelastic>
46       <S1_alpha_beta>...</S1_alpha_beta>
47     </CoherentInelastic>
48   </scatteringAtom>
49 </scatteringAtoms>
50 </thermalScattering>
51

```

Note: This option assumes the use of methods (e.g. density functional theory/lattice dynamics with 1-phonon corrections) for calculating the content of its data blocks (i.e. S , S_s and 1S_s).

Figure 4.3. An example of “Option 3” for the GNDS format of TSL data

```

1
2
3 <thermalScattering
4   material="U (UN) "
5   MAT="72">
6   <documentations>
7     <documentation style="endfDoc">
8       <documentation name="endfDoc"><![CDATA[
9         U (UN)      LEIP LAB      EVAL-SEP17 J.L. Wormald, A.I. Hawari
10        NDS 148, 1 (2018)      DIST-FEB18
11        ----ENDF/B-VIII.0      MATERIAL 72
12        -----THERMAL NEUTRON SCATTERING DATA
13        -----ENDF-6 FORMAT
14        Temperatures = 296 400 500 600 700 800 1000 1200 K
15
16        Background
17        -----
18        ...
19        ]]>
20     </documentation>
21   </documentations>
22   <scatteringAtoms>
23     <scatteringAtom label="0" numberPerMolecule="1">
24       <mass value="236.0058" unit="amu"/>
25       <CoherentBoundCrossSection value="9.283302" unit="b"/>
26       <IncoherentBoundCrossSection value="9.283302" unit="b"/>
27       <e_critical value="197.6285" unit="eV"/>
28       <e_max value="5.000001" unit="eV"/>
29       <coherentElastic>
30         <S_table>...<S_table>
31       </coherentElastic>
32       <IncoherentElastic calculatedAtThermal="true">
33         <DebyeWaller>...</DebyeWaller>
34       </IncoherentElastic>
35       <IncoherentInelastic>
36         <T_effective>
37           <axes>
38             <axis index="1" label="temperature" unit="K"/>
39             <axis index="0" label="t_effective" unit="K"/></axes>
40           <values>296 306.097 4e2 407.5307 5e2 ... 1200 1202.533</values>
41         </T_effective>
42         <Ss_alpha_beta>...</Ss_alpha_beta>
43       </IncoherentInelastic>
44       <CoherentInelastic>
45         <Sd1_alpha_beta>...</Sd1_alpha_beta>
46       </CoherentInelastic>
47     </scatteringAtom>
48   </scatteringAtoms>
49 </thermalScattering>
50

```

Note: This option assumes the ability of modern techniques (e.g. density functional theory/lattice dynamics with 1-phonon corrections) to calculate the content of its data blocks (i.e. S_s and S_d).

4.2. TSL uncertainties

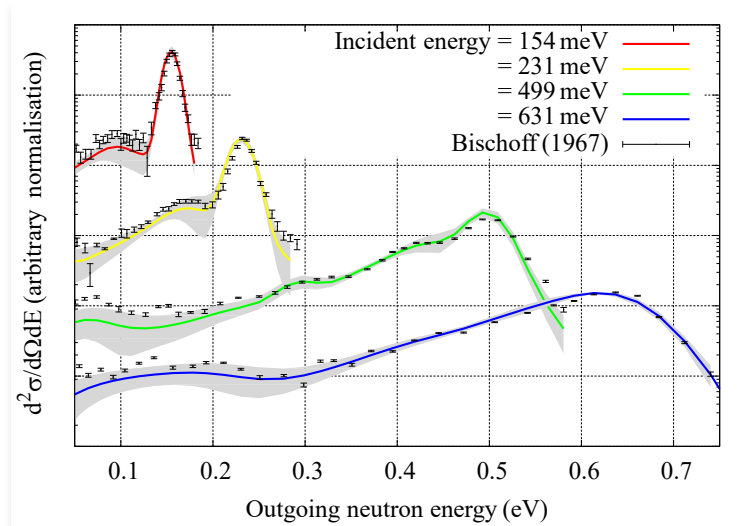
The ENDF-6 format does not allow for the storing TSL uncertainties. Consequently, neither covariance matrices nor well accepted procedures for computing covariances can be recommended to propagate TSL uncertainties in neutronic calculations. Several independent works have addressed such issues.

For light water, previous attempts for propagating uncertainties due to hydrogen cross-sections with the total Monte Carlo technique were mainly based on random TSL produced by varying the LEAPR parameters, assuming they are all independent. The technique was first applied to H in H₂O of the Joint Evaluated Fission and Fusion File (JEFF)-3.1.1 (Rochman and Koning, 2012). A slightly different approach was also proposed by Lance Maul and applied to the TSL of light and heavy water of ENDF/B-VIII.0 (Maul et al., 2018). This strategy relies on the phenomenological representation of the density of states (DOS) calculated by MD simulations.

A more elaborate Monte Carlo technique was proposed by Holmes and Hawari (2014). It consists of generating uncertainties by sampling an ab initio phonon frequency spectrum. In this case, the DOS was treated as a probability distribution function of available atomic vibrational energy states. For a solid material, density functional theory and lattice dynamics in the harmonic approximation can be used to simulate the structure and produce the DOS. A range for the variation in the DOS can be established based on limits of variation in lattice related parameters. Consequently, a description of possible variation in the DOS allows Monte Carlo generation of a set of perturbed DOS spectra, which are sampled to produce the $S(\alpha, \beta)$ covariance matrix for thermal scattering. With appropriate sensitivity matrices, the $S(\alpha, \beta)$ covariance matrix can be propagated to generate covariance matrices for integrated cross-sections, secondary energy distributions and coupled energy-angle distributions. It should be noted that this methodology may apply when using data derived from other techniques, including experiments.

TSL uncertainties for reactor applications were discussed in “Covariance matrices of the hydrogen neutron cross sections bound in light water for the JEFF-3.1. 1 neutron library” (Noguere et al., 2017; Scotta et al., 2017; Scotta et al., 2018) by using TSL of H in H₂O from JEFF-3.1.1 and ENDF/B-VIII.0 (namely CAB model in the papers). In both cases, the covariance matrix between the model parameters (LEAPR parameters for JEFF-3.1.1 and GROMACS (GRONingen MACHine for Chemical Simulations) parameters for ENDF/B-VIII.0) were generated with the CONRAD code by fitting experimental total cross-sections and average cosine of the scattering angle. A marginalisation procedure is used to account for systematic uncertainties. Double-differential neutron scattering cross-sections were not included in the fitting procedure. These data were only used to verify the consistency of the final results (see Figure 4.4). Covariances between multi-group $S(\alpha, \beta)$ and neutron cross-sections were calculated via the model parameter covariance matrix. The obtained uncertainties were propagated to reactivity coefficients calculated for critical assemblies operating in “cold” conditions (temperature below 80°C) and for pressurised water reactors in “hot” operating conditions (300°C). For uranium oxide (UOX) benchmarks, uncertainties on the calculated k_{eff} , due to TSL uncertainties of JEFF-3.1.1, are close to ± 130 pcm at room temperature and ± 50 pcm at 300°C. The low uncertainty obtained at high temperature confirms the weak impact of the TSL uncertainties in the reactivity uncertainty at “hot” operating conditions. In the case of the TSL of ENDF/B-VIII.0, the performance of the obtained covariance matrix has only been quantified on integral calculations at “cold” reactor conditions between 20°C and 80°C. For UOX fuel, the uncertainty on the calculated reactivity ranges from ± 71 to ± 155 pcm. For mixed oxide (MOX) fuel, it ranges from ± 110 to ± 203 pcm. At room temperature, for UOX fuel, Lance Maul also reports low uncertainties of about ± 50 pcm, confirming the good quality of the CAB model at $T=300$ K. However, for both UOX and MOX fuels, the increasing uncertainties on the calculated reactivity reflect the temperature-dependent bias observed in Figure 3.15.

Figure 4.4. **Double-differential scattering cross-sections for light water calculated with JEFF-3.1.1 (Mattes' model) and compared with data measured by Bischoff et al. (1967) at the Rensselaer Polytechnic Institute (RPI) facility**



Note: The grey areas represent the 1-sigma uncertainty bands calculated with the CONRAD code using the covariance matrix between the LEAPR parameters.

Source: Bischoff et al., 1967.

Works done on the TSL of light water offer the possibility of testing three different options in the future GNDS format, which consist of storing and communicating:

- covariance matrix between the LEAPR parameters;
- covariance matrix between the multi-group $S(\alpha_s, \beta)$;
- covariance matrix between the angle-integrated scattering cross-section.

Chapter 5. Summary and recommendations

Over the past 20 years, there has been renewed interest in the development of thermal scattering libraries to support the needs of the nuclear science and engineering community. Two databases were released in 2018: the Evaluated Nuclear Data File (ENDF)/B-VIII.0 and the Joint Evaluated Fission and Fusion File (JEFF)-3.3 (Brown et al., 2018; NEA, 2017). In the United States, the ENDF library, the majority of the new and/or updated thermal scattering law (TSL) libraries, are based on the use of the atomistic simulation techniques presented in this report. In the JEFF library, TSL for cold neutron moderators and neutron filters rely on experimental data. The new and updated TSL libraries, including the methods that supported the evaluation and the evaluating institution, are listed in Table 4.1 of this report.

The participants of the NEA Working Party on International Nuclear Data Evaluation Co-operation (WPEC)/Subgroup (SG) 42 presented experimental and theoretical contributions that are discussed in this report. In parallel, these groups made the single largest contribution to the thermal scattering sub-library in the history of evaluated nuclear data libraries, with 33 new and updated evaluations incorporated in the latest releases of ENDF/B and JEFF. In particular, new evaluations for nuclear graphite and light water ice were made as a result of user and regulatory demands.

Among the contributions was the identification and development of new computational tools aClimax/oClimax (ISIS), FLASSH, North Carolina State University), NCrystal (European Spallation Source [ESS]), NJOY (Los Alamos National Laboratory) that will help in solving future needs in thermal scattering data, and in the collaboration with WPEC SG 38 for the initial specification of the Generalised Nuclear Data Structure (GNDS) nuclear data format for storing the data. The participants also produced a wealth of new experimental data for the validation of scattering kernels and proposed methodologies for the quantification of uncertainties.

With this in mind, the subgroup makes the following recommendations:

- support the development of open source tools for thermal scattering data evaluation and processing with focus on providing nuclear data on demand at operational conditions;
- strengthen the collaboration with the neutron science and advanced neutron source communities (Spallation Neutron Source [SNS], ESS, Institut Laue-Langevin [ILL], ISIS) in each country to establish joint experimental programmes;
- support the data collection effort by EXchange FORmat (EXFOR) both in thermal scattering nuclear reaction data and supplementary material;
- identify and select sets of benchmark experiments that most appropriate for supporting the TSL evaluation process;
- converge on a modern format for TSL data in consultation with the GNDS effort;
- study the accuracy requirements for TSL evaluations, data processing and utilisation.

Consequently, during the last session of SG 42, the participants unanimously recommended the start of a follow-up subgroup to continue the co-ordination of the international effort in TSL development and evaluation. This recommendation was also supported by entire WPEC body in the meeting held on 20 May 2018.

References

- Abe, Y. and S. Tasaki (2015), "Molecular dynamics analysis of incoherent neutron scattering from light water via the Van Hove space-time self-correlation function with a new quantum correction", *Annals of Nuclear Energy*, Vol. 83, pp. 302-308.
- Abe, Y., T. Tsuboi and S. Tasaki (2014), "Evaluation of the neutron scattering cross-section for light water by molecular dynamics", *Nuclear Instruments and Methods in Physics Research Section A: Accelerators, Spectrometers, Detectors and Associated Equipment*, Vol. 735, pp. 568-573.
- Agostinelli, S. et al. (2003), "GEANT4: A simulation toolkit", *Nuclear Instruments and Methods in Physics Research Section A: Accelerators, Spectrometers, Detectors and Associated Equipment*, Vol. 506, No. 3, pp. 250-303.
- Atchison, F. et al. (2005), "Measured total cross sections of slow neutrons scattered by gaseous and liquid H₂", *Physical Review Letters*, Vol. 94, No. 21.
- Berendsen, H.J.C. et al. (1995), "GROMACS: A message-passing parallel molecular dynamics implementation", *Comput. Phys. Comm.*, Vol. 91, pp. 1-3.
- Bischoff, F. et al. (1967), *Low Energy Neutron Inelastic Scattering (LENIS) in Linear Accelerator Project Progress Report*, Technical Report RPI-328-27.
- Brown, D.A. et al. (2018), "ENDF/B-VIII. 0: The 8th major release of the nuclear reaction data library with CIELO-project cross sections, new standards and thermal scattering data", *Nuclear Data Sheets*, Vol. 148, pp. 1-142.
- Cai, Q. and A.I. Hawari (2012), "Neutron powder diffraction study of reactor grade graphite", *Embedded Topical Meeting on Nuclear Fuels and Structural Materials for the Next Generation Nuclear Reactors*, US.
- Cai, X.X. et al. (2018), "Rejection-based sampling of inelastic neutron scattering", *Journal of Computational Physics*, Vol. 380, pp. 400-407, <https://arxiv.org/abs/1808.02634>.
- Cantargi, F. et al. (2017), "Preliminary scattering kernels for ethane and triphenylmethane at cryogenic temperatures", *EPJ Web of Conferences*, Vol. 146, p. 13003. EDP Sciences.
- Celli, M. et al. (1999), "The total neutron cross section of liquid para-hydrogen", *Journal of Physics, Condensed Matter* 11, No. 50.
- CSEWG (2010), "ENDF-6 Formats Manual, Data Formats and Procedures for the Evaluated Nuclear Data Files ENDF/B-VI and ENDF/B-VII", edited by M. Herman and A. Trkov, CSEWG Document ENDF-102, Report BNL-90365-2009 Rev.1, National Nuclear Data Center, Brookhaven National Laboratory.
- Dritsa, M. and A. Kostikas (1967), "Total cross-section of water at room temperature and 20°C", EANDC (OR)-63L.
- Fougeras, P. et al. (1999), "MISTRAL-4: An experimental mockup in the EOLE facility devoted to high moderation 100% MOX core physics", *Proceedings of International Conference on the Future Nuclear Systems, GLOBAL'99*, US.
- Grammer, K.B. et al. (2015), "Measurement of the scattering cross section of slow neutrons on liquid parahydrogen from neutron transmission", *Physical Review*, B 91, No. 18.

- Hawari, A.I. (2014), "Modern techniques for inelastic thermal neutron scattering analysis", *Nuclear Data Sheets*, Vol. 118, pp. 172.
- Hawari, A.I. and B.W. Wehring (2014), "Observation of neutron thermalization in graphite using the slowing-down-time technique", *Proceedings of the International Conference on Physics of Reactors (PHYSOR 2014)*, 28 September to 3 October 2014, Japan.
- Hawari, A.I. and V.H. Gillette (2014), "Inelastic thermal neutron scattering cross sections for reactor grade graphite", *Nuclear Data Sheets*, Vol. 118, pp. 176-178.
- Hawari, A.I. et al. (2016), "Testing of a Thermal neutron scattering law for nuclear graphite in support of TREAT neutronic analysis", *Transactions of the American Nuclear Society*, Vol. 115, pp. 1401-1403.
- Hawari, A.I. et al. (2014), "Inelastic neutron scattering analysis of reactor grade graphite", *Embedded Topical Meeting on Nuclear Fuels and Structural Materials for the Next Generation Nuclear Reactors*, US.
- Hawari, A.I. et al. (2009), "Measurement of the total inelastic scattering cross section of graphite using 9 Angstrom neutrons", *Transactions of the American Nuclear Society*, Vol. 100, pp. 591-592.
- Hawari, A.I. et al. (2004), "Ab initio generation of thermal neutron scattering cross sections", *PHYSOR 2004: The Physics of Fuel Cycles and Advanced Nuclear Systems-Global Developments*.
- Holmes, J.C. and A.I. Hawari (2014), "Generation of an S (α , β) covariance matrix by Monte Carlo sampling of the phonon frequency spectrum", *Nuclear Data Sheets*, Vol. 118, pp. 392-395.
- Hügler, Th. et al. (2014), "Triphenylmethane, a possible moderator material", *Nuclear Instruments and Methods in Physics Research Section A: Accelerators, Spectrometers, Detectors and Associated Equipment*, Vol. 738, pp. 1-5.
- IAEA (2017), Thermal Scattering Law (TSL) Library Generation, www-nds.iaea.org/TSL-LibGen (accessed 1 September 2019).
- Kanaki, K. et al. (2018), "Simulation tools for detector and instrument design", *Physica B: Condensed Matter*, Vol. 551, pp. 386-389.
- Kasprzak, M. (2008), "Ultracold Neutron Converters", PhD Thesis, University of Vienna.
- Kittlmann, T. and M. Boin (2015), "Polycrystalline neutron scattering for Geant4: NXSG4", *Computer Physics Communications*, Vol. 189, pp. 114-118.
- Koppel, J.U. et al. (1967), "GASKET: A Unified Code for Thermal Neutron Scattering", Report GA-7417, General Atomics.
- Kresse, G. and J. Furthemüller (1996a), "Efficient iterative schemes for ab initio total-energy calculations using a plane-wave basis set", *Phys. Rev. B* 54, 11169.
- Kresse, G. and J. Furthemüller (1996b), "Efficiency of ab initio total energy calculations for metals and semiconductors using a plane-wave basis set", *Comput. Mater. Sci.* Vol. 6, pp. 1.
- Liu, M. and A.I. Hawari (2014), "Positron characterization of neutron irradiated reactor grade graphite", *Embedded Topical Meeting on Nuclear Fuels and Structural Materials for the Next Generation Nuclear Reactors*, US.
- MacFarlane, R.E. et al. (2017), "The NJOY Nuclear Data Processing System", Version 2016, LA-UR-17-20093, <https://permalink.lanl.gov/object/tr?what=info:lanl-repo/lareport/LA-UR-17-20093>.
- MacFarlane, R.E. (1994), "New Thermal Neutron Scattering Files for ENDF/B-VI Release 2", LA-12639-MS, <https://t2.lanl.gov/nis/publications/thermal.pdf>.

- Manring, C.A. and A.I. Hawari (2019), "Thermal neutron scattering in a heavy paraffinic molecular material", *Annals of Nuclear Energy*, Vol. 128, pp. 140.
- Márquez Damián, J.I. and V. Semkova (2015), *Summary Report of the Consultants' Meeting on Compilation of Thermal Neutron Scattering Data for Experimental Nuclear Reaction Data Library (EXFOR)*, IAEA-NDS Report INDC(NDS)-0697, www-nds.iaea.org/index-meeting-crp/CM-THSC-2015.
- Márquez Damián, J.I. et al. (2018), <https://github.com/marquezj/NJOY2016/tree/H2D2> (commit 783c030 on 12 April 2018).
- Márquez Damián, J.I. et al. (2016), "Generation of thermal scattering libraries for liquids beyond the Gaussian approximation using molecular dynamics and NJOY/LEAPR", *Annals of Nuclear Energy*, Vol. 92, pp. 107-112.
- Márquez Damián, J.I. et al. (2015), "Measurement of the total cross section of heavy water in the 0.1 meV-1 eV energy range at 20 and 50°C", *Proceedings of UCANS-V, Il Nuovo Cimento-C*, Vol. 178, p. 6.
- Márquez Damián, J.I. et al. (2014), "CAB models for water: A new evaluation of the thermal neutron scattering laws for light and heavy water in ENDF-6 format", *Annals of Nuclear Energy*, Vol. 65, pp. 280-289.
- Mattoon, C.M. et al. (2012), "Generalized nuclear data: A new structure (with supporting infrastructure) for handling nuclear data", *Nuclear Data Sheets*, Vol. 113, No. 12, pp. 3145-3171.
- Maul, L. et al. (2018), "Perturbation scheme for estimating uncertainties in thermal scattering cross sections of water", *Annals of Nuclear Energy*, Vol. 121, pp. 232-249.
- Mukherjee, M. et al. (1998), "Spectral frequency distribution for liquid deuterium determined by neutron scattering", *Physical Review*, B 57, no. 18, American Physical Society.
- NEA (2017), *JEFF 3.3 Nuclear Data Library*, www.oecd-nea.org/dbdata/jeff/jeff33.
- Noguere, G. et al. (2017), "Covariance matrices of the hydrogen neutron cross sections bound in light water for the JEFF-3.1.1 neutron library", *Annals of Nuclear Energy*, Vol. 104, pp. 132-145.
- Parlinski, K. et al. (1997), "First-principle determination of the soft mode in cubic ZrO₂", *Phys. Rev. Lett.*, Vol. 78, 4063.
- Plimpton, S. (1995), "Fast parallel algorithms for short-range molecular dynamics", *J. Comput. Phys.*, Vol. 117, pp. 1.
- Ramić, K. (2018), *From Experiments to DFT Simulations: Comprehensive Overview of Thermal Scattering for Neutron Moderator Materials*, PhD dissertation, Rensselaer Polytechnic Institute.
- Ramić, K. et al. (2018), "Thermal scattering law of C₂H₄n: Integrating experimental data with DFT calculations", *Annals of Nuclear Energy*, Vol. 120, pp. 778-787, <https://doi.org/10.1016/j.anucene.2018.06.029>.
- Ramirez-Cuesta, A.J. (2004), "oClimax4.0.1, The new version of the software for analyzing and interpreting INS spectra", *Computer Physics Communications*, Vol. 157, Issue 3, pp. 226-238, doi:10.1016/S0010-4655(03)00520-4.
- Roach, D.L. et al. (2013), "The interpretation of polycrystalline coherent inelastic neutron scattering from aluminium", *Journal of Applied Crystallography*, Vol. 46, pp. 1755-1770.
- Rochman, D. and A.J. Koning (2012), "Random adjustment of the H in H₂O neutron thermal scattering data", *Nuclear Science and Engineering*, Vol. 172, No. 3, pp. 287-299.

- Santamarina, A. (1989), "Thermal effects analysis in LWR lattices – Thermal cross-section shapes and qualification through French integral experiments", IAEA TECDOC-491.
- Scotta, J.P. et al. (2018), "Generation of the 1H in H₂O neutron thermal scattering law covariance matrix of the CAB model", *EPJ Nuclear Sciences and Technologies*, Vol. 4, p. 32.
- Scotta, J.P. et al. (2017), "Towards a covariance matrix of CAB model parameters for H (H₂O)", *EPJ Web of Conferences*, Vol. 146, p. 13010, EDP Sciences.
- Scotta, J.P. et al. (2016), "Impact of the thermal scattering law of H in H₂O on the isothermal temperature reactivity coefficients for UOX and MOX fuel lattices in cold operating conditions", *EPJ Nuclear Sciences and Technologies*, Vol. 2, pp. 28.
- Shibata, K. et al. (2011), "JENDL-4.0: A new library for nuclear science and engineering", *J. Nucl. Sci. Technol.*, Vol. 48(1), pp. 1-30.
- Squires, G.L. (1978), *Introduction to the Theory of Thermal Neutron Scattering*, Cambridge University Press, Cambridge.
- Stepanov, S.B. et al. (1974), "Temperature dependence of total cold neutron cross section in light water and benzene", *Soviet Atomic Energy*, Vol. 37, No. 4, pp. 1094-1096.
- Van Hove, L. (1954), "Correlations in space and time and born approximation scattering in systems of interacting particles", *Physical Review*, Vol. 95, pp. 249-262.
- Walley, S.P. et al. (2016), "Measurement of positive temperature coefficients of reactivity for rack-like arrangements of reactor fuel in the neptune zero energy facility", *Proceedings of the European Research Reactor Conference (RRFM)*.
- Willendrup, P. et al. (2004), "McStas 1.7 a new version of the flexible Monte Carlo neutron scattering package", *Physica B*, Vol. 350, E735.
- Yamamoto, T. et al. (1997), "Core physics experiment of 100% MOX core MISTRAL", *Proceedings of International Conference on Future Nuclear Systems, Japan, GLOBAL'97*.
- Young, J.A. and J.U. Koppel (1964), "Slow neutron scattering by molecular hydrogen and deuterium", *Physical Review*, Vol. 135, No. 3A, American Physical Society.
- Zhu, Y. and A.I. Hawari (2018), "Reactor physics paving the way towards more efficient systems", *Full Law Analysis Scattering System Hub (FLASSH), PHYSOR 2018, Mexico*.
- Zoppi, M. et al. (1996), "Structure factor of compressed liquid deuterium close to the melting transition", *Physical Review*, E 54, No. 3.

NEA PUBLICATIONS AND INFORMATION

The full **catalogue of publications** is available online at www.oecd-nea.org/pub.

In addition to basic information on the Agency and its work programme, the NEA website offers free downloads of hundreds of technical and policy-oriented reports. The professional journal of the Agency, **NEA News** – featuring articles on the latest nuclear energy issues – is available online at www.oecd-nea.org/nea-news.

An **NEA monthly electronic bulletin** is also distributed free of charge to subscribers, providing updates of new results, events and publications. Sign up at www.oecd-nea.org/bulletin.

Visit us on **Facebook** at www.facebook.com/OECDNuclearEnergyAgency or follow us on **Twitter** @OECD_NEA.



Thermal Scattering Law $S(\alpha, \beta)$: Measurement, Evaluation and Application

Understanding the nature of neutron scattering in various media at operating temperatures, whether they be reactor fuels, cryogenically cooled neutron sources or any materials at room temperature, is an essential component in the modelling of all nuclear systems. Neutrons that reach these energies, which are millionths of the initial fission and spallation neutron energies, cause virtually all of the fission that occurs in present reactors, including in Generation III+ designs, as well as in several designs that are being proposed for future reactors. As part of a broad range of co-operative activities in basic nuclear science, the Nuclear Energy Agency (NEA) is supporting collaboration between experimentalists, theoreticians and modelling experts to advance the state of the art in nuclear data.

This report reviews progress made by the NEA Working Party on International Nuclear Data Evaluation Co-operation (WPEC) Subgroup on Thermal Scattering Kernel Measurement, Evaluation and Application, which brought together a full spectrum of relevant experts to advance the state of the art in thermal scattering law data. The collaboration resulted in 33 new material evaluations, including uranium nitride (UN), silicon carbide (SiC), silicon oxide (SiO_2) and aluminium oxide (Al_2O_3), as well as the re-evaluation of critical materials such as water (H_2O) and heavy water (D_2O), and enhanced evaluations of "nuclear" graphite at multiple levels of porosity and of phase I_n ice. Nuclear data libraries have adopted these data for their most recent releases – including the new Evaluated Nuclear Data File (American) and Joint Evaluated Fission and Fusion (NEA Data Bank) – which are being used around the world as international standards.